

**Development of a Molecularly Imprinted
Polymer (MIP)-based sensor platform for the
fast and low-cost detection of yeast and
pathogenic bacteria**

N MansouriBoroujeni

Masters of Science (by Research)

2017

Development of a Molecularly Imprinted Polymer (MIP)-based sensor platform for the fast and low-cost detection of yeast and pathogenic bacteria

By: Negar MansouriBoroujeni

A thesis submitted in fulfilment of the requirements of the Manchester Metropolitan University for the degree of Master of Science (by Research)


Department of Chemistry

Manchester Metropolitan University

Master of Science (by Research)

“I declare that the work detailed here has not been submitted for any other award at Manchester Metropolitan University or any other Institution.”

“I declare that, except where specifically indicated and referenced in this word, all the work presented in this report is my own and I am the sole author of all parts. I understand that any evidence of plagiarism and/or the use of unacknowledged third part data will be dealt with as a very serious matter”

Signature  29.10.17

Date: 24-Oct-2017

Text Word Count: 13914

Overall word count: 14698

Abbreviation:

AA	Acrylamide
AIBN	2,2'-Azobis(2-methylpropionitrile)
AMR	Antimicrobial resistance
CV	Cyclic voltammetry
DMSO	Dimethylsulfoxide
FTIR	Fourier-transform Infrared Spectroscopy
MAA	Methacrylic acid
MIP	Molecularly Imprinted polymer
MRSA	Methicillin-Resistant Staphylococcus aureus
NIP	Non Imprinted Polymer
NMR	Nuclear magnetic resonance spectroscopy
PPY	Polypyrrole
SEM	Scanning Electron Microscopy
SPE	Screen printed electrode
TRIM	1-[2-(trifluoromethyl)phenyl]-
HTM	Heat Transfer Method
PBS	Phosphate Buffer Solution
WLS	White Light Scanner

Abbreviations	iv
Project tile	1
Summary	1
1. Introduction	3
1.1 MIP and NIP	4
1.2 Free Radical Polymerisation of MIP	5
1.3 Escherichia coli	6
1.4 Yeast	8
1.5 MRSA	8
1.6 Antibiotics	9
1.7 Electrodes	10
1.8 Functional Monomer: Pyrrole	13
1.9 Heat Transfer Method (HTM)	16
2. Project Aims	18
3. Experimental	18
3.1 Testing The Potentiostat	18
3.2 PBS	19
3.3 PPY synthesis	19
3.4 Choosing an Electrode	20
3.5 yeast MIP and NIP preparation	20
3.6 PBS Using Tablets	21

3.7 MIP modified removal technique	21
3.8 Aminophenol Electro- Polymerisation	21
3.9 Aluminium Electrode Experiments	22
3.10 Initial Yeast Experiments in the HTM Set Up	24
3.11 SEM Imaging of Yeast SPEs	25
3.12 Preparation of MRSA MIP and NIP Using Emstat	26
3.13 Yeast MIPs on Gold	28
3.14 Bulk Polymerisation	29
3.15 E. coli MIP and NIP	31
3.16 NMR measurements	32
4. Results and discussion	32
4.1 PPY Synthesis results	32
4.2 Finding the Optimum Electrode	36
4.3 Yeast MIP and NIP UV-Vis	37
4.4 Aminophenol Gold and SPE results	38
4.5 Aluminium Electrode polymerisation results	40
4.6 FTIR AI Results	41
4.7 White Light Scanner Results and Explanation	43
4.8 HTM SPE Graphs	45
4.9 SEM images on SPEs and explanations	49
4.10 MRSA MIP and NIP results	53
4.11 MRSA and E. coli Microscope Pictures after Staining	57

4.12 Yeast Gold HTM Results	58
4.13 Bulk Polymerisation Tables and Graphs of Results	61
4.14 E. coli MIP and NIP results via the HTM	64
4.15 NMR data of pyrrole	66
5. Conclusions	68
6. Future Work	71
7. Acknowledgments	72
8. References	73
9. Appendix	a

Project Title:**Development of a Molecularly Imprinted Polymer (MIP)-based Sensor Platform for the Fast and Low-Cost Detection of Yeast and Pathogenic Bacteria****Summary:**

A protocol for electro-polymerisation was first developed for polymers that can specifically detect *Saccharomyces cerevisiae* (yeast) and subsequently expanded to polymers for the analysis of different strains of MethicillinResistant *Staphylococcus aureus* (MRSA) and *Escherichia coli* (*E.coli*). Molecularly Imprinted

Polymers (MIPs) were deposited on the surface of electrodes (respectively ScreenPrinted Electrodes, gold and aluminium electrodes) using electrochemical methods. Parameters that were varied included the voltage, polymerization time, and monomer concentration. Cyclic Voltammetry (CV) was used to evaluate the polymerization process by monitoring the oxidation and reduction peaks of the monomers. The surface architecture of the MIPs differs with the type of electrodes that were used, which was studied with Scanning Electron Microscopy and Infrared analysis. Subsequently, to obtain high affinity binding sites on the MIP layer, extraction had to be performed. This protocol was first developed for yeast and subsequently adapted to fit with the removal of pathogenic bacteria (which requires use of Class II lab facilities). The developed MIP-SPEs were inserted into a homemade thermocouple device and exposed to various solutions of the target concentrations. For MIPs for yeast, an increase in the thermal resistance was measured after target bound to the polymer recognition layer. This is a first indication that we can use thermal detection methods, such as the Heat-Transfer

Method, to determine and quantify microorganisms in buffered solutions. In the future, this will be extended to

MIP-based thermal sensors for the detection of pathogenic bacteria. Advantages of these thermal sensors are their low-cost and that they allow for rapid and simple analysis, which makes them a valuable and versatile analytical tool.

1. Introduction

Molecularly Imprinted Polymers (MIPs) are artificial receptor ligands, which can recognize and specifically bind their target molecules and are used as synthetic receptors.

Molecularly Imprinted Polymers (MIPs) have either nano or micro sized cavities that imprint the specific alignment and positioning of functional groups that are present on the surface of the substrate or the template.¹ MIPs are the ideal tool for the detection of molecules or some small cells in a biological sample (blood plasma) due to their capability to bind to specific substrates similar to an enzyme. However, harsh physical conditions such as temperature and pH certainly denature enzymes; MIPs are more structurally stable and are able to resist to such conditions allowing them to remain selective towards the substrate.²

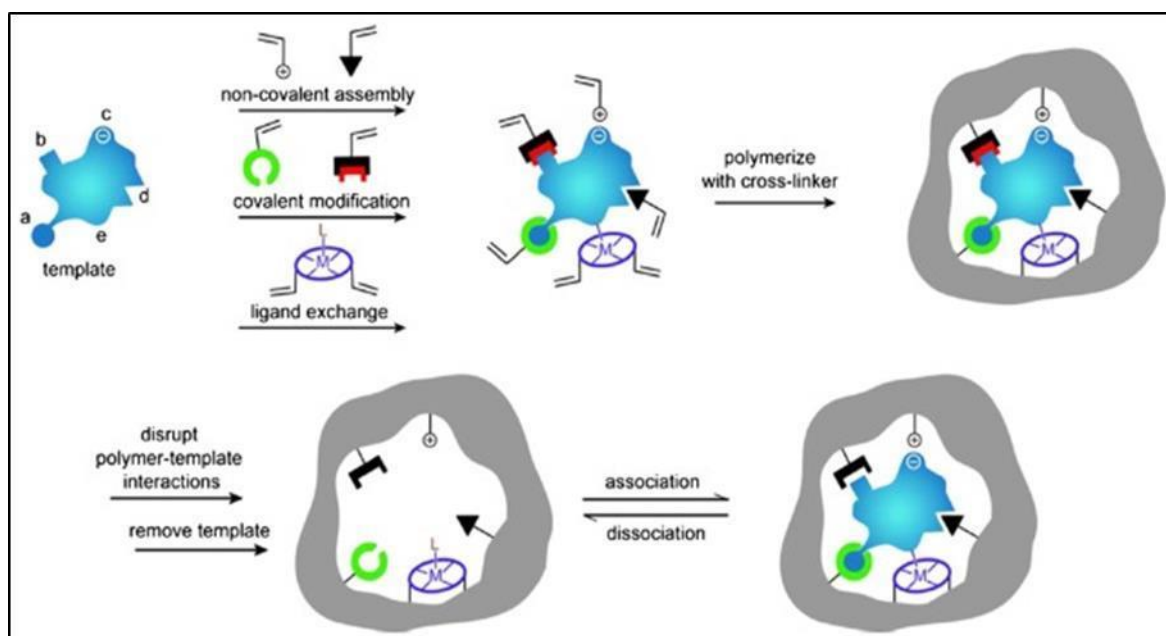


Figure 1 Schematic illustration of MIP polymerization (see reference Fig1)

The figure above displays how the template molecule is able to bind to the different monomers making the template monomer-complex. After polymerization and

removal of the target molecule, this gives the MIP its distinct high affinity cavities, also known as the polymer matrix.

In the last years, there is a tendency to move towards these 'plastic' receptors as they mimic enzyme-ligand affinity but have superior thermal, chemical and longterm stability. In addition, these recognition elements can be prepared in bulk quantities and are cost-effective compared to other separation techniques that are commonly used, (for example High Performance Liquid Chromatography), which gives them a high commercial potential. MIPs can be reused and stored for long periods while they continue to maintain their receptor properties. In addition, they possess excellent chemical and thermal stability and can be used in a wide range of temperatures and pH levels.³ There are two types of MIPs, based on covalent and non-covalent interactions. Non-covalent MIP rely on the ionic and other chemical interaction (excluding covalent bonds) that could occur between the polymers and the target molecule, also known as the template. These interactions are reversible, which allows MIP- based sensors to be used many times as long as the template is extracted after each rebinding.⁴

Hence, the overall intention is to develop target specific-MIP micro-particles and implement them into biosensors for the detection of biological toxic agents such as viruses or pathogenic bacteria that cause many diseases and death due to the environmental contamination.

1.1 MIP and NIP

A Non Imprinted Polymer (NIP) is synthesised in exactly the same manner as the MIP, but with the exception that polymerization occurs in the absence of the target molecule. The NIP will not contain the micro or nanocavities that are present in the

MIP and can therefore not bind the template with high affinity. Therefore, this will be used to serve as a reference and in order to evaluate the specificity of the developed MIPs.

1.2 Free radical polymerization of MIPs

MIPs are traditionally prepared *via* free radical polymerization. This means target, monomer and crosslinker molecules are dissolved into a suitable porogen. This porogen should not interfere with the interactions between the target and the monomer (pre-polymerization complex) and should be able to create pores into the MIP microstructure. Subsequently, an azo-compound is added to initiate polymerization *via* UV light or *via* heat. This generates a radical that are transferred to the monomer, and subsequently the polymer chain starts to grow. Termination occurs through combination of two free radicals or *via* disproportionation reactions.¹ Since this is a free radical polymerisation, there is no control over the length of the chain. This means that a broad molecular weight distribution is formed and a heterogeneous mixture of the MIP binding sites. The created structure will result in micro particles that are subsequently ground and sieved prior to incorporation into the sensor electrodes (average size of 2-5 micron).

Functionalization of these microparticles onto electrodes is not straightforward and requires the use of an additional adhesive layer, such as polyvinylchloride (see *A MIP-based sensor for the Impedimetric Detection of Low Molecular Weight Molecules by VanSweevelt and Thoelen et al*). However, disadvantages of this procedure include that this is time-consuming and a maximum surface coverage of 30% is obtained.

During electro polymerization a small film or layer of polymer is formed over the surface of an electrode. This is caused by the potential that is applied to the electrode. The voltage and the time it takes for the polymer layer to form depends

on the functional monomer in electropolymerisation. The advantages of this procedure include that it is fast, polymerization can be controlled by adapting the voltage and time, and it is possible to confirm a monolayer and thereby significantly increase surface coverage. In addition, instead of microparticles, nanosized layers are obtained that have superior thermal properties which will have a positive impact on the limit of detection of those sensors.

During this study, a non-imprinted polymer was tested against the MIP to check for the polymer's ability to isolate the specific template. Reaction conditions such as formulation of MIP reaction mixture including choice of cross-linking monomer, functional monomer, and porogenic solvent, reaction temperature, and time altogether govern the properties, physical appearance, morphology, and performance of powder MIPs.

The first batch of bulk polymers were made for yeast and then followed by antibiotics, the functional monomer was altered depending on the ionic bonds needed in the MIP cavities.

1.3 Escherichia coli

Escherichia coli (*E. coli*) is a Gram-negative, rod-shaped, facultative anaerobic bacterium. This microorganism was first described by in 1885.⁵ Most *E. coli* strains harmlessly colonize the gastrointestinal tract of humans and animals as normal flora. However, there are some strains that have evolved into pathogenic strains and they most commonly lead to severe food poisoning as well as meningitis and infections. A high level of resistance to antibiotics has been found across several strains of *E. coli* but it is rare to find these strains causing illness.⁶

Because of the potential severity of infections caused by *Escherichia coli* O157, it is important that very sensitive laboratory methods are used both for outbreak investigation and surveillance. Selective culturing of *E. coli* O157 remains the

detection method of choice, but this is time-consuming (48 h for conventional culture methods), Alternatives to culture include immunoassays and PCR, both of which are available as commercial detection kits but are expensive and require sophisticated lab environments.⁷ The last 15 years has seen many advances in detection of E. coli O157 and this has been accompanied by a plethora of reports in the scientific literature. ⁷ However, it is an area which is continually developing and we are still far away from a universally accepted method for this purpose.⁶

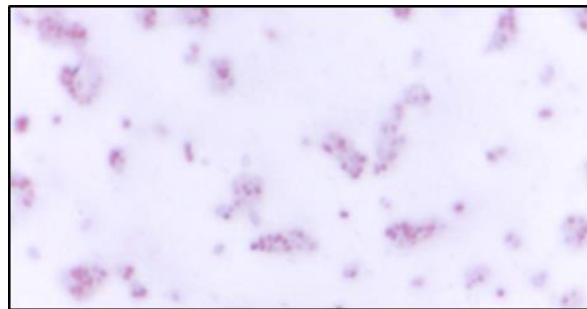


Figure 2 *Picture of a culture of E.coli taken with a light the microscope after staining in the microbiology labs*

1.4 Yeast

The protocol for this study will be developed using baker's yeast first. Yeast is available from supermarkets and is low-cost and easy to manipulate. Yeast is classified as a Class I organism and therefore it is not necessary to work in the Class II lab facilities of Microbiology. However, as it is very similar to mammalian cells, it is very suitable to be used as a model organism. Therefore, optimization studies were conducted with yeast before moving to Class II organisms

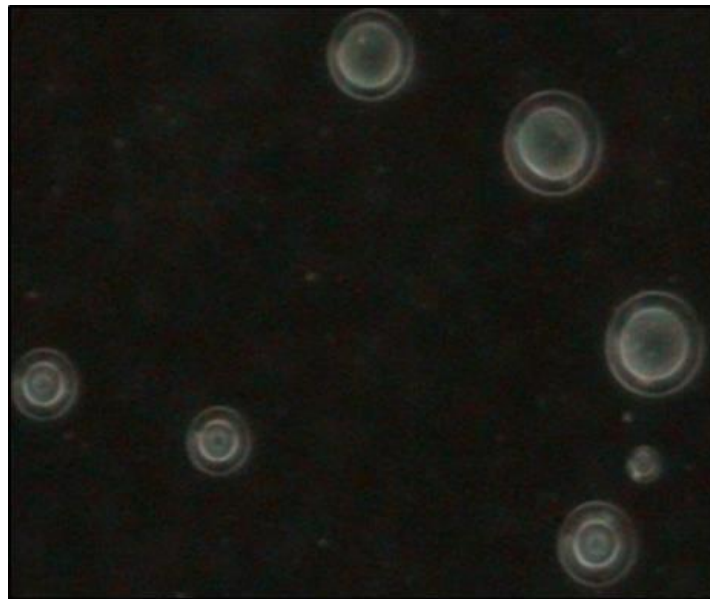


Figure 3 *Picture of yeast taken using a light microscope*

1.5 MRSA

MRSA is a common and often deadly bacterium that causes skin, lung, and heart infections. According to literature the cases of (MRSA) Methicillin-Resistant *Staphylococcus aureus* are on the rise and they are increasingly becoming more and more resistant to antibiotics.⁸

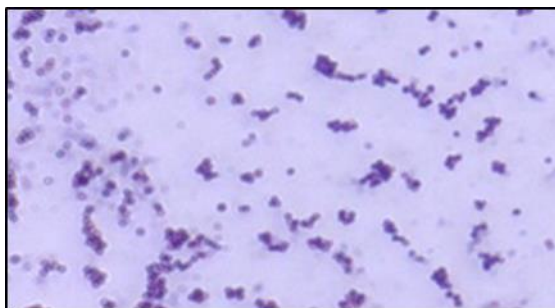


Figure 4 *Picture of a culture of MRSA strain '252' taken with a light microscope after staining in the microbiology labs*

In this study 3 different strains of MRSA were examined and used as the target molecule in the electropolymerisation process. The MRSA strains were then used for HTM analysis. The different strains were used as competitor templates to test if the MIP synthesised was selective to a specific strain.

1.6 Antibiotics

Rational selection antibiotics: **Amoxicillin and Nafcillin**

According to a recent WHO report, antibiotic resistance should be regarded as a global threat comparable to climate change and terrorism.⁹ Most concerns about antibiotic resistance are linked to acquired resistance, which makes a bacterial subpopulation resistant to a certain drug or group of drugs because of genetic changes. It is accepted that use of antibiotics in veterinary or clinical practice exerts a selective pressure, which accelerates the emergence and propagation of antibiotic resistance. The mostly used antibiotic classes in veterinary medicine, and antibiotic residues found in aquatic environments, belong to the beta-lactams, fluoroquinolones, macrolides, sulfonamides, and tetracyclines.¹⁰ Therefore, we will evaluate the use of MIP sensors for Amoxicillin and Nafcillin, which are common antibiotics from the beta-lactam class.¹¹

Polymers for the two penicillin based drugs were made during this research and they electrochemical properties of these polymers were observed together with the polymers for bacteria.

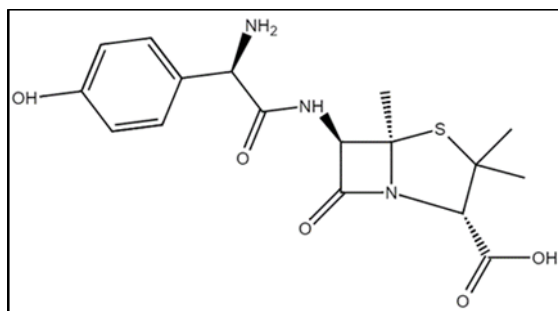


Figure 5 Structure of Amoxicillin

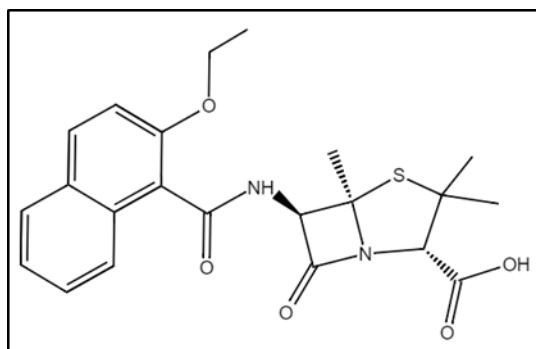


Figure 6 The structure of Nafcillin

1.7.1 Electrodes

Initially, three different working electrodes were tested for the polymerization of pyrrole to examine which one would be a better suited electrode and to determine the differences of the polymers made by each electrode.

1.7.2 Glassy Carbon Electrodes



Figure 7 *Picture of a Glassy Carbon electrode*

The copper wire at the top of the electrode is connected to the clips attached to the potentiostat.

Glassy carbon electrodes are non-graphitizable carbon which combines glassy and ceramic properties with those of graphite. The graphite part at the end of the electrode is the part that is suspended in the solution for electro polymerisation.

The tips need to be carefully polished using grid paper before use.

1.7.3 Screen Printed Electrodes (SPEs)

Screen printed graphite electrodes are more recently being used as an alternative to traditional larger electrodes.

SPEs are disposable and easily printed on ether paper or polyester and very cost effective compared to other electrodes.

The screen printing process of these simple electrodes has the aptitude for the mass production of highly reproducible electrodes. The volume of polymer layer on the SPEs was found to be the smallest of all the electrodes that were examined; this is because the surface area that the polypyrrole takes place of the SPEs is much smaller therefore the oxidation and reduction peaks of the pyrrole recorded during a cyclic voltammetry scan were also much shorter. However, it was decided to use the SPEs mainly throughout the research due to them being readily available and cheaper and less likely to get damaged compared to other electrodes. SPEs

are also easier to analyse after the polymerisation, for example, they were cut down and coated with gold for SEM imaging.



Figure 8 Picture of a SPE printed by Chris Foster (Banks group) according to the procedure detailed in reference (Fig 8)

These SPEs consisted of a three-electrode configuration with a 3-mm graphite working electrode, graphite counter electrode and Ag/AgCl pseudo-reference electrode. SPEs were fabricated in-house using a microDEK 1760RS screenprinting machine (DEK, Weymouth, UK). The ink that was used was a carbongraphite ink formulation (Product Code C2000802P from Gwent Electronic Materials) and was printed onto a polyester substrate.¹² (*More information about the procedure can be found in reference 12*).

1.7.4 Gold and other metallic based electrodes

The metallic electrodes are 1 cm to 1 cm squares that fit perfectly into the HTM set up. Gold-coated silicon electrodes provide a high surface area and displayed sharp oxidation and reduction peaks in the CV graphs, which makes them better suitable for electrochemical detection. In addition, the surface is smoother compared to the SPEs and this enabled to obtain clear SEM images of the MIP (before and after rebinding and template removal) and the NIP to determine the polymer surface architecture.

1.7.5 Counter electrode

In a system like a potentiostat, three electrodes (*working, counter and reference electrodes*), are used for electrochemical measurements. The current when a

potential is applied between the working and reference electrode is measured. An electron transfer reaction is required between the counter and the working electrodes for the passage of current through an electrical circuit. Therefore, the counter electrode is used to provide the site of the second electron transfer reaction. The main purpose of the counter electrode is the important parameter of the surface area in the reaction. For the potentiostat experiments, a graphite counter electrode was used.

Model: Graphite counter electrode 23 cm

The experiments carried out by the Emstat (*a smaller version of the potentiostat/ pictures included in the appendix*), used screen printed electrodes as counter electrode, due to the smaller sensors and smaller vial or beaker used for these experiments. The SPEs used as counter were then disposed of.

1.7.6 Reference Electrode

A reference electrode has a well-known electrode potential which is stable. The reference electrode in electrochemical studies, works as a redox. For the experiments using the potentiostat, a silver/ silver chloride reference electrode was used. The equilibrium in the redox was between the metal (Ag) and its salt (AgCl).

SPEs were used for the experiments using the Emstat yet again, due to their size being more suitable.

1.8 Functional monomer:

Functional monomers used in this study were pyrrole and aminophenol, due to the reason that both chemicals are capable of ionic polymerization that results in the NH surface bond needed to synthesise MIPs and NIPs for yeast and the bacteria. According to the literature that was found and the short initial experiments (further

discussed later), it was found that pyrrole had a much shorter polymerization time and is able to polymerize at neutral pH. Therefore, it was chosen as the main monomer for this research.

Pyrrole

Pyrrole is a donor heterocyclic aromatic compound with symmetry along the y-axis according to microwave spectroscopic measurements. Pyrrole appears as a light gold transparent liquid that darkens when it is exposed to air. Pyrrole also turns into a black brownish more solid colour in the process of polymerisation. It is also known by its IUPAC name N-methylpyrrole, $C_4H_4NCH_3$. Although it is not a naturally occurring compound, many of the derivatives of pyrrole can be found in natural molecules, and mostly commonly, they are found in the Heme B molecule and chlorophyll¹³.

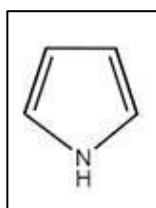


Figure 9 The structure of pyrrole

Pyrrole molecules are prepared by reacting ammonia with furan molecules; this method is most commonly used for industrial purposes. This reaction is an example of the Paal-Knorr synthesis¹⁴, as shown in the reaction below:

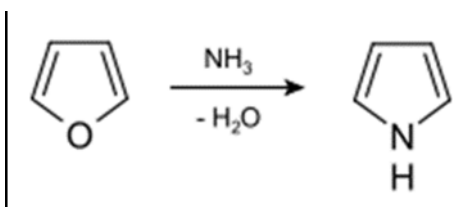


Figure 10 Structure reaction of furan with ammonia resulting in pyrrole.

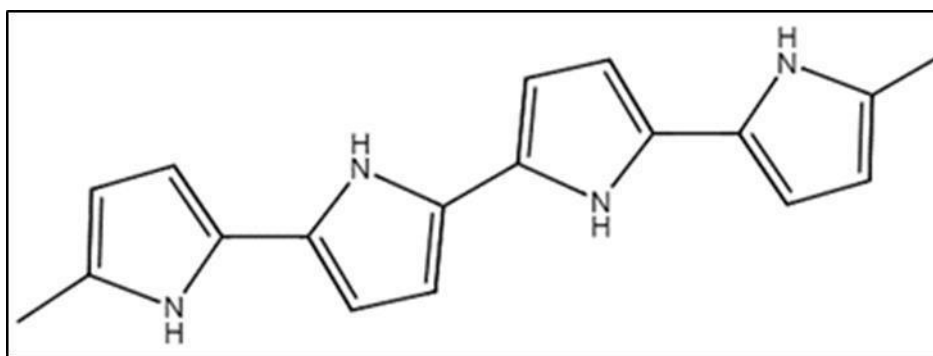


Figure 11 Picture of the structure of polypyrrole (PPY)

Polypyrrole (PPY) is formed by the polymerisation of pyrrole, which occurs naturally by simple exposure to the air.¹⁵ However, it occurs much faster electrochemically in the presence of a constant potential.¹⁵ The PPY layer is usually yellow but darkens over time to a black or a dark brown colour. The thicker the film layer is the darker it appears. PPY is described as "quasi-unidimensional" vs onedimensional since there is some crosslinking and chain hopping.¹⁵

The application of PPY in recent years has been popular in the areas of electronic devices and the usage in chemical sensors. More current studies have proposed to use PPY as a potential vehicle for drug delivery.¹⁵ It is known that the polymer matrix can act as a vessel for proteins or other targets. This principle was used in this study; the ionic bonds formed due the NH region on the polypyrrole are able to bind to surface sites on yeast and the surface proteins of the cell wall of the bacteria such as MRSA.

Substituted derivatives such as N-methylpyrrole are also called pyrroles. Pyrrole and its derivatives are widely used as an intermediate in synthesis of pharmaceuticals, dyes and perfumes (and other organic compounds). For example, chlorophyll, heme are the derivatives which are made by four pyrrole ring formation of porphyrin ring system; they are used as catalysts for polymerization process, corrosion inhibitors, preservatives, and as solvents for resins and

terpenes.¹⁶ Some derivatives of pyrrole are also have been examined to have antibiotic properties. Molecules like, pyoluteorin¹⁶ and 1,2-Di(4-pyridyl) ethylene both have been investigated to be active against bacterial. However, most studies show that these antimicrobial properties are mostly active in vitro rather than in vivo (according to studies carried out on mice). Additionally, it has been reported that the toxicity of the pyrrole derivative molecule has hindered its antimicrobial properties.¹⁷

1.9 Heat Transfer Method (HTM)

The Heat-Transfer Method (HTM) is used to detect the rebinding of the yeast, MRSA and E. coli to the MIP-functionalised sensor.¹⁸ Once bacteria are bound to the surface, heat flow is blocked in a certain direction and a difference in the temperature is picked up by the device. This is used to quantify the amount of yeast/bacteria bound to the surface.

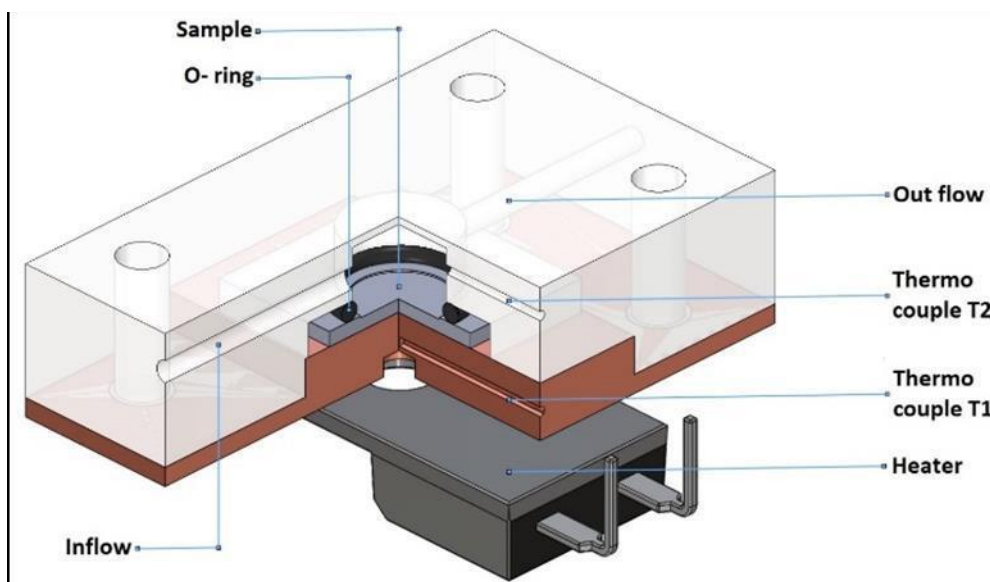


Figure 12 Picture representing the Heat flow cell

Figure 12 shows a schematic representation of the components forming of the HTM flow cell with internal volume of 110 μL . The main components are the two

thermocouples T_1 and T_2 , one measures the temperature at the heat sink that is actively controlled (T_1) and the other measures the temperature in the liquid that is merely monitored (T_2). The sample are MIP-functionalized electrodes, either on SPEs or on gold, that are connected to the heat sink. The thermal resistance heatflow encounters are determined by the temperature gradient between T_1 and T_2 .¹⁸ A Proportional Integral Derivative (PID) controller is used to keep T_1 at a constant temperature.¹⁹

Easy manipulation of the adherence of solute passing through the solution inside the flow chamber to the internal surfaces will affect the functionalization of the surface and the corresponding heat resistance.

By changing the PID settings, the level of control on the temperature stability is varied and this affects the standard deviation on the measurement signal. As this is directly linked to the limit of detection (defined at the concentration at which the effect equals three times standard deviation on the baseline signal), it is very important to optimize PID settings of measurements.

The temperature T_2 is solely monitored and any changes at the solid-liquid interface will be reflected in the temperature of the liquid. To eliminate any external effects, the thermal resistance is determined rather than observing the effect in temperature. The thermal resistance (R_{th}) is calculated by dividing the temperature gradient ($T_1 - T_2$) over the input power at the heat resistor. In this project, we will measure the response of functionalized MIP-SPEs to different concentrations of targets, and attempt to construct a dose-response curve for quantification purposes¹⁶.

2. Project Aims

The project aims for this study are listed below:

Initial aim of this study is to develop a protocol for the electro-polymerization of MIPs that have a high affinity for a particular yeast strain. Subsequently, by optimizing the conditions (time, voltage, monomer used and its concentration) we will move towards MIPs specific to pathogenic strains.

The final aim is to develop target specific-MIP micro particles and implement them into biosensors for the detection of biological toxic agents such as viruses and bacteria. We will focus on this project on thermal detection and use a thermocouple device that was patented by the group of Dr. Peeters.

3. Experimental

3.1 Testing the Potentiostat

For this project two devices were used for the electro polymerization process, initially the first half of these processes were carried out using the potentiostat; *Model Autolab PGSTAT302N*.

To a dried volumetric flask (100 mL) a mixture of KCl (7.5 g, 1 mM) followed by potassium ferro-cyanide (0.0329 g, 1 mM) was added and dissolved in deionised water.

Three electrodes, including a counter electrode, a reference electrode and a working electrode, were attached to the sensors connected to the potentiostat. Via the programme **Nova 2.0** a cyclic voltammetry reading of the ferrocyanide solution was recorded, a linear reading was taken with the voltage of 1+ V to check to see if the oxidation and reduction peaks for the solution were present at that voltage.

*NOVA 2.0 is the new electrochemistry software from Metrohm Autolab. This application is used to control all compatible Autolab devices and equipments. NOVA 2.0 combines the power and flexibility of the preceding versions with a simple and modern operator interface. NOVA 2.0 uses a graphical demonstration that is consistently used in the application.*²⁰

3.2 Phosphate Buffer Solution (PBS)

A 100-mL solution of 0.2 M phosphate buffer was prepared at pH 7:

To a clean and dried (100 mL) volumetric flask the following were added respectively; 16 g NaCl, 0.49 g of KCl, 2.88 g of Na₂HPO₄, 0.48 g of monopotassium phosphate (KH₂PO₄) and deionised water. The resulting solution was mixed and stirred until all components were fully dissolved.

Using a pH probe the initial pH was noted at pH 6.89, the original pH was used because it was found to be optimum pH required for this experiment (according to the researched literature).²¹

3.3 Polypyrrole (PPY) synthesis

PPY film was prepared by applying a constant potential of + 0.98 V. 1 mmol (0.6709 g) of pyrrole was weighed out and added to a 100 mL of 0.2 M phosphate buffer solution.

For 60 to 90 seconds the positive voltage was applied to the system and a linear graph of the polymerisation was produced via the potentiostat.²¹⁻²²

PPY formed a thin black layer on the surface of the working electrode, which was mostly visible on the Au electrode.

3.4 Choosing a working electrode

Three working electrodes were tested originally as the working electrodes to determine which of the electrodes would have been better suited for the study including glassy carbon, SPEs and gold.

1 mmol of pyrrole was added and dissolved in the PBS (100 ml).

About 25 mL of the solution was poured into a small beaker, the sensor part of the electrodes were suspended in the solution held in place using clips. The electrodes were attached to the potentiostat and a cyclic voltammetry (CV) reading with 5 scans of each electrode was taken (changing the pyrrole mixture every time the electrode was altered).

3.5.1 Yeast MIP and NIP preparation

A yeast Eppendorf tube (concentration measured at 460 nm) was drained of its growth medium and washed in PBS three times using a centrifuge for the process. The yeast sample was then transferred using an automated pipette into 1 mL of PBS and added to a dry volumetric (100 mL flask) containing 100 ml of PBS and pyrrole solution previously made, this was used as the MIP

100 mL of the PBS containing 1mL pyrrole solution (excluding the yeast) was kept as the NIP.

Different SPEs were used for the MIP and NIP, 2 SPEs were polymerised at 60 s and 2 were polymerised at 90 s. A CV scan of each electrode was logged (with the potential parameters ranging from -1.2 Vs to 1.6 Vs) to check the oxidation and reduction peaks of pyrrole.

The SPEs were then dried using an air flow and stored in labelled vials.

3.5.2 Yeast MIP repeats and Removal of template using acid

The method above was repeated again. This time, the imprinted SPEs were dipped into a 0.1 M solution of NaOH prior to the drying process.

3.6 PBS solution using tablets (SIGMA)

One tablet dissolved in 200 mL of deionized water yields 0.01 M phosphate buffer, 0.0027 M potassium chloride and 0.137 M sodium chloride, pH 7.4, at room temperature.²³ Tablets were placed in a small beaker containing 20 mL of distilled water and sonicated for fast dissolving then the solution was transferred to a 200 mL volumetric flask and made up.

3.7 MIP and NIP of yeast and new modified removal technique

After the previous SPEs were analysed they appeared to be damaged due to the dipping in the strong base solution. The gold layer clearly peeled off and the dark blue/black silicon layer became visible. A new improved removal process of the template was developed. After polymerisation, the SPEs were washed cautiously in hot water and the dried and stored in labelled vials.

3.8 Aminophenol Electro-polymerisation

Into a dried volumetric flask, a 100 mL p-aminophenol solution was prepared by adding 0.1 M nitric acid (HNO_3), and 6.5 mM of aminophenol. The mixture was degassed using nitrogen gas for 2 to 3 minutes. This was kept as the NIP. The same process was repeated and 1 mL of yeast was added to the solution, which corresponded to the MIP.

According to previous research, it was found that aminophenol electropolymerisation takes up to 3 hours at the constant potential of -1.3 V.²⁴

25 mL of the MIP followed by the NIP were taken for the polymerisation process. At first gold electrodes were used for the electropolymerisation but it was discovered that because of the presence of the acid, the gold top layer on the gold silicon electrodes was fading away. The experiment was then repeated with SPEs. After the three-hour linear sweep of the electropolymerisation, a CV graph was recorded from each electrode (with the potential parameters ranging from -0.1 Vs to -1.3 Vs)

3.9.1 Aluminium Experiments

Aluminium electrodes were polished with sand paper and subsequently cut into 1cm squares. These electrodes were used as a cheaper alternative to the gold ones. Due to the flatter metallic surface (which is much smoother than the uneven graphite based surface of the SPEs) they were used in the polymerisation using both aminophenol and pyrrole polymers.

3.9.2 FTIR using an ATR

Fourier Transform Inferred spectroscopy (FTIR) technique was used to determine at what exact time the PPY single layer film was fully formed on the surface of the electrodes. FTIR provided high spectral resolution data over a wide spectral range. To begin with 5 different SPEs were used until it was found that the graphite on the SPEs interfered with the IR readings. Therefore, the method was altered to use Al electrodes instead.

5 Al electrodes were used for this part of the experiment. A solution of 1 mM pyrrole in 100 mL PBS (pyrrole NIP) was made. Electrode number one was simply dipped in the solution and left to dry. The 2nd electrode was polymerised electrochemically for the duration of 30 seconds. The third one was then polymerised for 60 s,

followed by the next one that was polymerised for 90 s and the final electrode was polymerised for 120 seconds.

The IR spectrum of all of the electrodes was taken using the FTIR which will be discussed later in the results part of the paper.

3.9.3 White Light Scanner

Three Al electrodes were polished with sand paper and washed with hot distilled water and dried. A small piece of parafilm was used to cover half of the electrodes. This is crucial for white light measurements since it needs to determine the difference in height between a “bare” electrode and polymerized part. Pyrrole MIP and NIP solutions were used to electropolymerise 2 SPEs for containing the MIP and 1 covered with the NIP. One of the MIP electrodes was removed of its template by washing the yeast in hot water and drying. The parafilm was then removed resulting in an electrode that was only partially electropolymerised. The white light scanner was used to take surface images of each electrode. The height of the MIP continuing the temple, the NIP layer and the MIP with its template removed was calculated using those images.

However, it was difficult to determine how much the surface of the aluminium had interfered with the size of the polymer monolayer because the Al electrodes contain small cuts and scratches from being polished with sand paper in the cleaning process.

The experiment was then repeated using 4 gold electrodes to obtain more accurate data.

3.10.1 Initial experiments of yeast in the HTM set up

The Heat Transfer Method was used for the rebinding of the yeast (the target molecule) to the MIP. A SPE functionalized with pyrrole, of which the yeast was extracted from the surface, was cut into a 1 cm to 1 cm square and then was mounted in the thermal set up of Dr. Peeters. It was mounted onto a copper block, which was stabilized for an hour at a temperature of 37.00 °C. During the measurement, the sample was first stabilized in PBS (because the yeast was washed in and kept in PBS) and then the same concentrations of yeast as the polymerisation was added. A graph was provided that showed the thermal resistance (R_{th}), which is defined as the temperature gradient between the copper and the fluid divided over the power (P). Changes at the solid-liquid interface, such as binding of yeast, have a pronounced effect on the thermal resistance.

As a reference a blank SPE was mounted in the HTM set up with the same conditions as discussed above. No significant effect was observed when a concentration of yeast was added to the electrode and therefore it was concluded no binding occurred at the surface.

Both SPEs were washed with PBS and the HTM set up was flushed with PBS, the MIP signal returned to baseline but the black one did not.

3.10.2 HTM of MIP and NIP yeast

One of the previously made MIP SPEs was cut into a 1 cm to 1 cm square for the sensing experiment in the HTM set up.

It was flushed with PBS and stabilised for 1.5h at the temperature of 37 °C with the HTM set up inside an incubator so that the environmental change (for example opening the door to the lab or the air conditioning) would no effect the experiment.

Increasing concentrations of yeast were added starting with the lowest first (ranging from 1000 times diluted to 100 times 50 times diluted, 10 times diluted and 1 mL of yeast). The concentrations were made using small automated pipettes in the microbiology lab and kept on ice, each sample of yeast was first vortexed before injection to make sure the yeast did not all sink to the bottom of the vial.

Each sample was added over a 5 minute long injection *via* a pump that was beforehand set up to the HTM system, with an hour long gap between each injection for stabilization of the R_{th} value.

The experiment was then repeated with the NIP electrode for comparison of the rebinding between the two polymers.

3.11 SEM imaging of the yeast SPEs

Coating of samples is mandatory in the field of electron microscopy to enable or improve the images. Creating a conductive layer of metal on the sample inhibits charging, reduces thermal damage and improves the secondary electron signal required for topographic examination in the SEM.²⁵

Sputter coating for SEM is the process of applying an ultra-thin coating of electrically-conducting metal – such as gold (Au), gold/palladium (Au/Pd), platinum (Pt) or silver (Ag) onto a non-conducting or poorly conducting specimen. Sputter coating prevents charging of the specimen, which would otherwise occur because of the accumulation of static electric fields. Sputtered films for SEM typically have a thickness range of 2–20 nm.²⁵⁻²⁶

The polymerized part of the SPEs were cut into small circles placed on metal buttons and labelled. They were then sputter coated with gold and argon gas using a rotary supper coater ready for SEM imaging.²⁷

3.12.1 Preparation of MRSA MIPs and NIPs using the Emstat (PSTrace 4.4)

Three different strains of MRSA bacteria (*provided by Prof Mark Enright, grown in MMU microbiology*) were washed out of the petri dishes into 10 ml vials containing the medium growth and left in an incubator for 24 h at 37 °C. 2 X 1 ml sample of each strain were transferred into PBS using the same procedure previously mentioned for yeast for the making of the MIPs.

The Emstat was connected to a laptop; the polymerisation took place via the program called 'PSTrace 4.4'. Screen printed electrodes were used as the working, counter and reference electrodes linked to the sensors of the Emstat placed in a small glass beaker. The beaker containing the MRSA sample mixed in PBS, a 1 mM pyrrole solution was mixed in the solution (a non-imprinted electrode was also polymerized as a reference). Each electrode was polymerized followed by a CV reading with 3 scans. MIPs were first cut to the preferred size, the working SPE electrode was placed in a labelled glass vial after drying. Prior to drying the electrodes imprinted electrodes were washed with hot water for the removal of the template.

Emstat: *The EmStat series are the smallest potentiostats available on the market.*²⁴

PSTrace 4.4: *Is the PC software used for the Cyclic Voltammetry (CV) and Linear Sweep Voltammetry (LSV) via the Emstat instead of the Potentiostat.²⁸*

3.12.2 Killing of the MRSA

The different concentration of the MRSA and all the SPEs (including the ones that were polymerised), were placed in an Ultra Violet Oven and they were left there for 3 minutes to kill of the bacteria so that they could then be used in the HTM set up and to prevent any contamination to the rest of the lab. This is because the lab where our research was performed is not of containment level II, and it is not possible to allow to detect microorganisms there.

3.12.3 MRSA and HTM

The three strains of MRSA used are named 252, C344 and C720 and are all cultured and grown in MMU Microbiology laboratory. At first, the thermal resistance was measured when the electrodes were exposed to solutions with increasing concentrations of MRSA. It was attempted to construct a dose-response in order to quantify MRSA levels in the solution. The different concentrations were prepared by diluting the MRSA mixtures from a stock solution. It was found that the binding of the templates took place to the MIP took place, which was observed as a significant increase in the thermal resistance. This rebinding was due to the fact that the MIP contains nanocavities with a similar size, shape and chemical functionality as the original template. Therefore, a 252 MIP electrode cut to 1 cm to 1 cm size was positioned in the HTM for a dose-response measurement. After addition of two solutions containing the same strain, a different strain of MRSA (C720) was injected to test the selectivity of the MIPs.

3.12.4 Staining of the MRSA and E. coli

Oil free microscope slides were washed using soap and warm water, wiped with alcohol, dried, and placed in laboratory towels until they were used. The slides were labelled on the underside using a glassware-marking pen. Using a sterile spatula, a small sample of the broth culture was placed in the middle of the slides. In a circular motion, the sample was smeared to about a centimetre in diameter. By means of a sterile spatula a drop of distilled water was placed on the smear, another small sample of the culture was smeared on top of the water drop resulting a in an emulsion.

After the smear was air dried, it was then passed through the flame of a Bunsen burner two to three times with the smear side up to kill off any contamination and the heat also killed off the bacteria which allowed for better staining.

The slides placed on the staining tray, the smear was at first gently flooded with crystal violet and let stand for 1 minute. Slides were slightly rinsed with sterile water using a wash bottle, the smears were then drowned mildly with Gram's iodine and left for another minute washed with water again. The purple stain was then decolourised using 95% ethyl alcohol or acetone, and then slanted and applied with the alcohol drop by drop (for about 5 to 10 seconds) until the alcohol ran clear followed by an immediate quick rinse with water. The slides were then washed with safranin to counter stain the smear and left to sit for 45 seconds. The tilted slides were eventually washed with water again and blot dried with bibulous paper. The smear was then viewed using a light microscope under oil immersion.

3.13.1 Yeast MIPs on gold electrodes

The same protocol as used earlier for the polymerisation was used at this point with a gold electrode. The gold electrodes were used in the HTM set up and the thermal response was compared to that of the SPEs.

3.13.2 White light scanner of Gold electrodes

Using the white light scanner, the following samples were analysed and 3D images were taken to determine the level of the thickness layer of the MIPs and NIPs:

- A MIP sample before extraction

- MIP sample after extraction that was covered in half by a Parafilm layer (to prevent polymerization)
- MIP after rebinding using the HTM that was covered in half by a Parafilm layer (to prevent polymerization) to be able to compare the part with polymer layer and the part that are just gold surface
- NIP after rebinding using the HTM that was covered in half by a Parafilm layer (to prevent polymerization) to be able to compare the part with polymer layer and the part that are just gold surface

The findings are explained in the results and discussion part of this study.

3.14 Bulk polymerisation of pyrrole

The first step was to take the IR reading of the materials and chemicals. This, in addition to $^1\text{H-NMR}$ of the synthesized compounds, was used to determine whether the samples were dry and if extraction of the template was complete.

The template molecule (1 mmol pyrrole) was dissolved in the porogen (DMSO 3 ml). The functional monomer (MMA 1.9 mmol), the cross-linker (acrylamide 5.3 mmol) and the initiator (AIBN 5.5 mmol) were added step by step. The pH of the mixture was not changed. The solution was degassed with a soft flow of N_2 . Polymerization was carried out in a silicone oil bath with the temperature monitored at around 75 degrees and left for 12 hours. After polymerization the brownish super solid polymers were grounded up and filtered. The polymers were then extracted to remove the template molecule 3 times using reflux each taking place for 12 hours. A non- imprinted polymer was also synthesised using the same method minus the template.

-
- At first the extraction occurred using a 50 ml mixture of 1:1 methanol and water
Followed by an extraction of 1:2 methanol and water
- Followed by an extraction of hot water only

The powered MIP and NIP were then dried in an oven at the 80 °C overnight. This section of the experiment was carried out in two parts.

A calibration graph of pyrrole was primary obtained at wavelength 210 nm, the observed wavelength for pyrrole according to literature.²⁹ A 1 M stock solution was made of pyrrole for the calibration, small glass vials were used. The stock solution was added to the vials and the different concentrations of pyrrole and diluted by adding distilled water the concentrations were 0.1, 0.3, 0.5, 0.6, 0.8 and 1 M and they were analysed from lowest to highest concentration to obtain the absorbance of pyrrole at different concentrations.

Secondly, the template molecule was added back to the MIP and the mixture then studied by UV-VIS spectroscopy. In this part, two sets of smaller glass vials were used each containing 3 ml of the different concentrations of pyrrole beforehand made. In one set 10 mg of MIP powder was added to each glass vial, and the other set consisted of 10 mg of NIP powder in each glass vial. This resulted in the formation of suspensions that were put in the orbital shaker (100 rpm) for 1 h. Subsequently, the polymer particles were filtered off until a clear solution was obtained that was measured with UV-vis.

Both sets were analysed using UV-Vis spectroscopy and the results were recorded using Excel and transferred into two graphs.

3.14.1 Bulk Polymerisation of yeast

The powered polymerisation of yeast was similar to the polymerisation of pyrrole, with the following materials used:

-

- 1 ml of yeast in PBS (same preparation technique as before) as the template

- 3.5 ml DMSO
- 30 mg of pyrrole as the functional monomer
- 1.02 g cross-linker (TRIM)
- 20 mg of AIBN as the initiator

The mixture then left in an oil bath at the temperature 65 °C for 5 hours, a NIP was also synthesised. The MIP and NIP were then washed and extracted in a reflux using hot water for 5 hours. The powdered were dried in an oven overnight at 70 °C. The extracted MIP wastewater was analysed under the microscope to see if the yeast extraction was complete. Optical batch rebinding experiments were performed to determine how much yeast bound to the MIP and its respective NIP.

3.14.2 Bulk polymerisation of antibiotics

The same protocol used for the bulk polymerisation of yeast, was again used here for the polymerisation of antibiotic: amoxicillin, with the exception of instead of using yeast as the template a 70 mg sample of amoxicillin was used as the template for the synthesis of the MIP.

3.15.1 E. coli MIP and NIP synthesis and 'Killing' process

Using a modified version of the method used for the analysis of MRSA was used here. Two strains of E. coli proved by Professor Mark Enright were used to make MIPs electrodeposited onto SPEs.

CV scans were taken during the polymerization via the Emstat and recorded in Excel. The same procedure was used to kill off the deadly bacteria to avoid contamination of the HTM set up.

•

The strains of E. coli used were grown and cultured in MMU were named:

- 10215
- 23849

3.15.1 E. coli thermal detection using HTM

Both MIPs were used to determine dose-response curves of E. coli in solution. 10215 was analysed and after a few injections of solutions with increasing concentration a different strain (23849) was added. Results are later discussed in more detail.

3.16 NMR measurements

NMR of pyrrole and the bulk polymers were taken using low-field NMR machine.

4. Results and Discussion

4.1 PPY Synthesis results

Using the method explained in section 3 of the report, SPEs were used for the polymerisation of pyrrole (1 M) in PBS. Six SPEs were used and each one was polymerised for a different duration: 5s, 30 s, 45 s, 60 s, 90 s and 120 s. Graphs of each polymerisation was recorded in excel the polymerisation took place via the Potentiostat using the graphite electrode as the counter electrode and the Ag/AgCl electrode as a reference electrode. Polymerisation graphs obtained from this experiment are called: voltammetry linear sweep graphs (VLS). The VLS graphs measure the current at the working electrode, while the potential between the reference and the working electrodes are logged in time (s), linearly (*figure 13*).

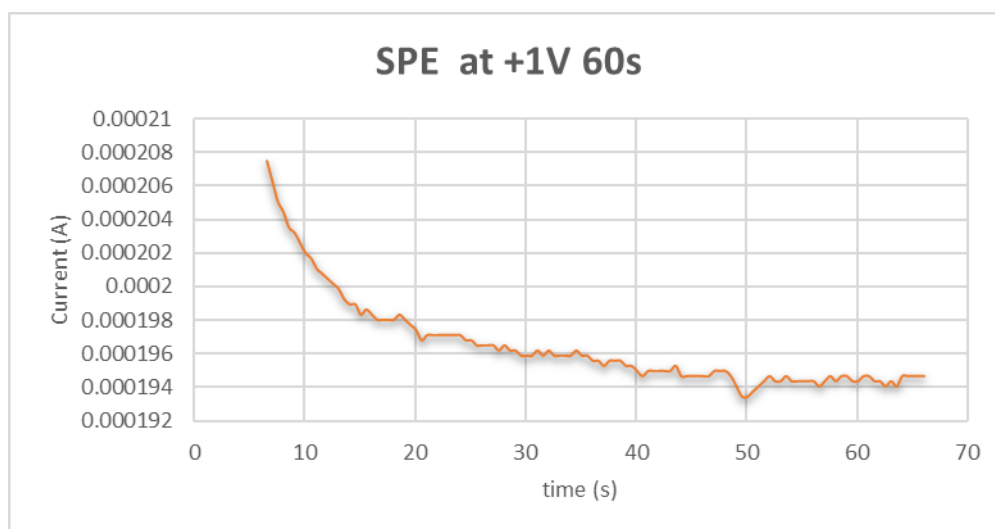


Figure 13 The VLS of SPE polymerised with PPY in 60 s

The linear sweep in figure 13 shows an example of one of the screen-printed electrode, polymerised for the duration of 60 s, using polypyrrole as a functional monomer.

The polymerised working electrodes are then connected to the sensors of the Potentiostat again and returned to the solutions they were polymerised in. A cyclic voltammetry (CV), graph is obtained from them (*using the same counter and reference as before*).

The CV is a technique used in electrochemical measurements, which allows for the sweeping of the electrode potential between parameters (E1 and E2), at a known sweep rate or scan rate. The sweep is reversed to accomplish a cyclic scan. Unlike the linear sweep where the voltage is kept the same throughout, in a CV voltage is set to two limits, V1 and V2. During the sweep when the voltage reaches V2, the scan is then reversed and swept back to V1.

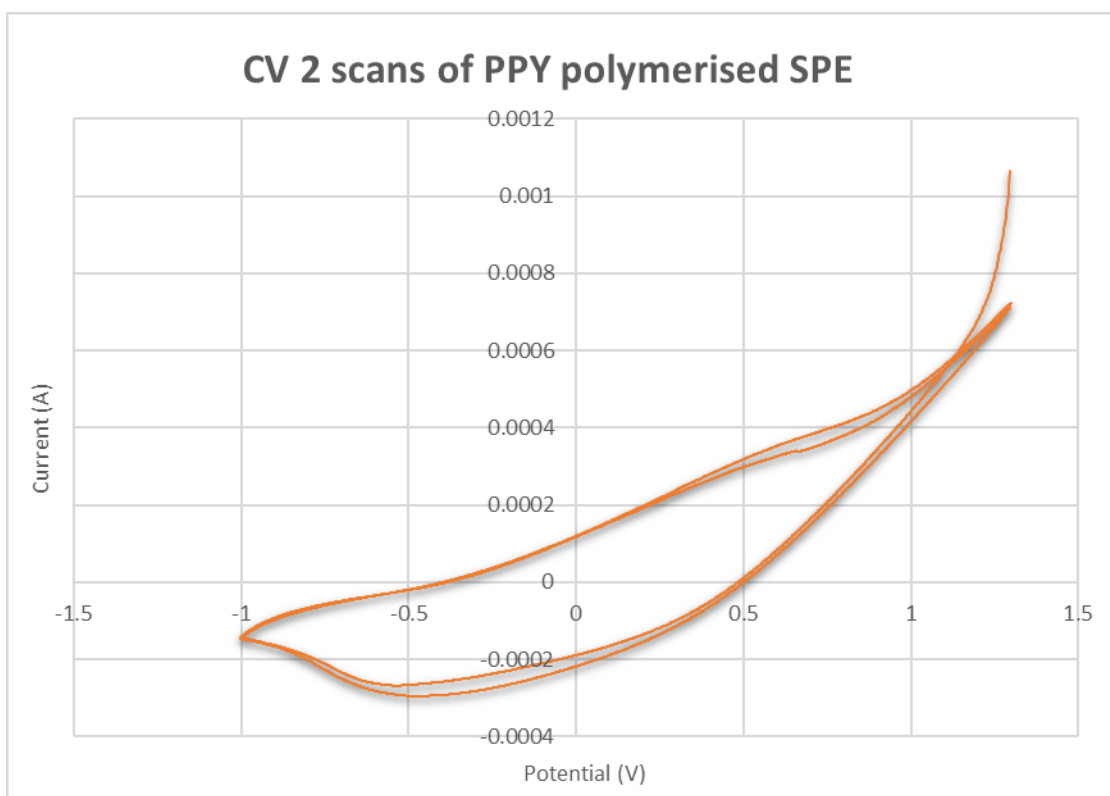


Figure 14 CV graph of PPY on SPE

Figure 14 is the graph of CV measurements taken from a SPE that was polymerised with PPY. According to the cyclic graphs above and further measurements the reduction peaks are observed to be around -0.6 V and the oxidation peaks are detected at around 0.4 V, these findings correspond to the literature previously found.¹⁵ The 2nd scan shows a slight shift in the position of the peaks, this could be due to the build of the polymer layer over time it has taken for the CV scans. It is known and observed in some parts of this study that pyrrole can self-polymerises without the presence of the potential and it uses oxygen to do so.¹⁵

Figure 14 is the graph of CV measurements taken from a SPE that was polymerised with PPY. According to the cyclic graphs above and further measurements the reduction peaks are observed to be around -0.6 V and the oxidation peaks are detected at around 0.4 V, these findings correspond to the literature previously found. The 2nd scan shows a slight shift in the position of the peaks, this could be

due to the build of the polymer layer over time it has taken for the CV scans. It is known and observed in some parts of this study that Pyrrole can self-polymerise without the presence of the potential and it uses oxygen to do so.

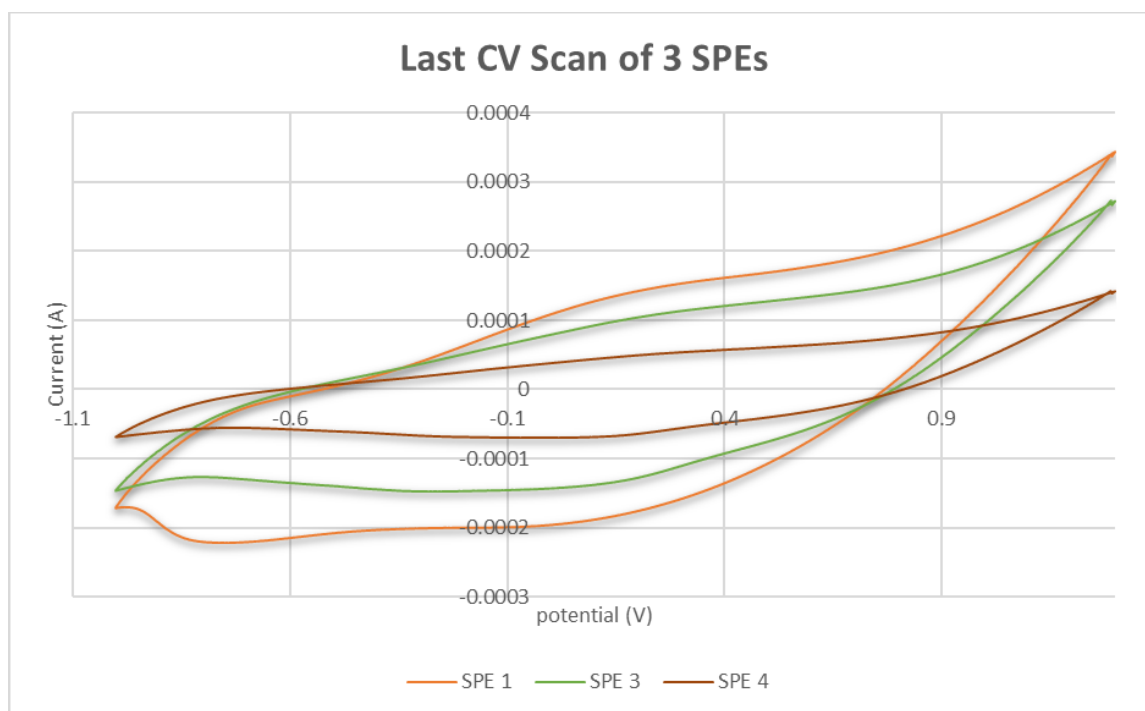


Figure 15 Graph depicting the CV scans of different polymerised SPEs showing the evidence of pyrrole (Five SPEs were used here, the three that showed the most clear peaks were used for this graph, SPE 1, SPE 3 and SPE 4)

CV scans showed the presence of pyrrole on the electrode, as clear oxidation peaks were observed in the spectra. According to the cyclic voltammetry graphs above the reduction peaks are observed to be around -0.6 V and the oxidation peaks are detected at around 0.4 V, these findings correspond to the literature previously found. The different SPEs used here clearly show that the concentration of PPY on each electrode is different, but fortunately, both the oxidation and reduction peaks are available on each scan.

4.2 Finding the Optimum Electrode

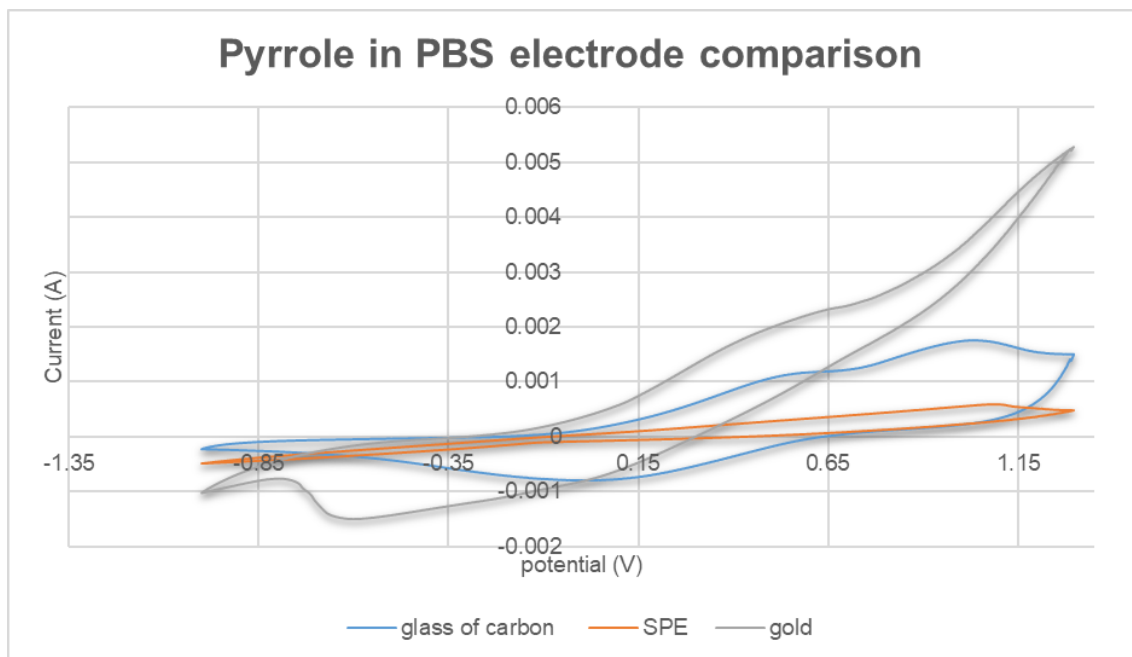


Figure 16 Graph depicting the CV graphs of the three electrodes after the polymerisation of pyrrole (60s) in PBS

As it was mentioned before the reduction peaks of pyrrole are typically around the -0.6 V area of the graph and the oxidation peaks are around 0.2 V to 0.4 V. The graph above is suggesting that sharper peaks are visible *via* the gold electrode compared to the others, and similarly, sharper peaks are observed *via* the glass of carbon electrode compared to the SPE. Therefore, the higher the surface area of the electrode, the higher concentration of polypyrrole is obtained, resulting in much sharper peaks. This graph is evidence that gold and other metallic electrodes (for example, aluminium), are much better suited electrodes to observe electrochemical activates. However, the metallic electrodes are much more expensive than the SPE and they need to be rigorously cleaned before use. For this study, both SPEs and gold electrodes were chosen for the HTM measurements and SEM imaging. Gold and aluminium electrodes were chosen for the analysis of the polymer surface

structures. When concentrations are increasing, the peaks are observed to shift slightly broadly, as detected on the graph above.

The integration of the area under the curve in the CV graphs can be calculated to determine the concentration of polypyrrole present at either the oxidation point or the reduction point.

4.3 Yeast MIP and NIP UV-Vis

The SPEs used for yeast were polymerised for 60 s, the CV graphs of them were then recorded.

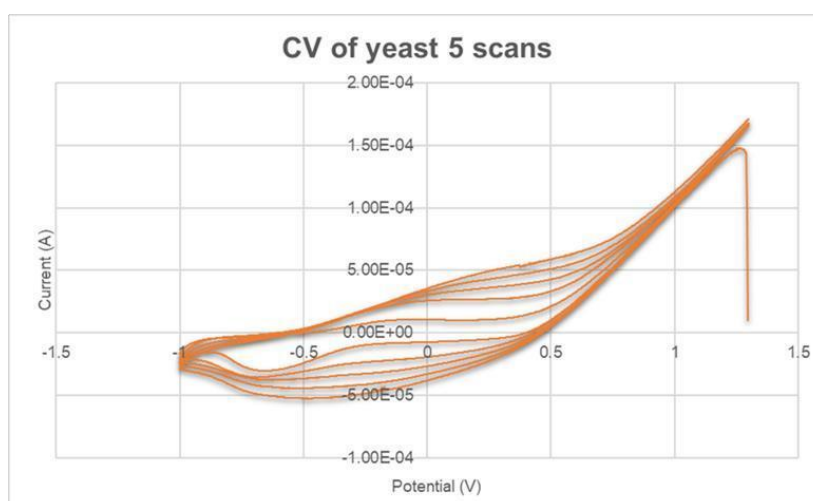


Figure 17 Five CV scans of SPE of yeast and PPY before extraction

The graph above suggest that the presence of yeast has shifted the oxidation and reduction peak slightly.

Using the methd that was mentioned before the yeast were extracted of the SPEs using hot water and dried using nitrogen gas and air. The CV scans of the yeast extracted SPEs were taken again. These SPes were now ready for the HTM set and for the rebinding of yeast

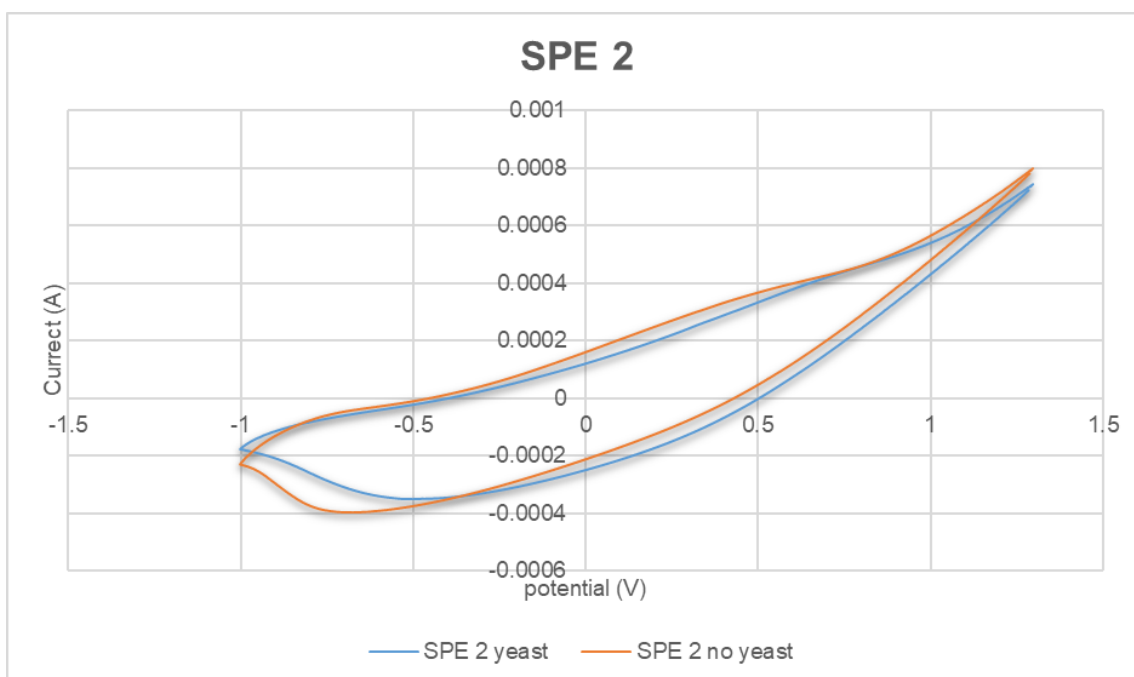


Figure 18 Comparing of the CV scans of before and after yeast extraction on SPE number 2

The graph shows a slight shift between the two sweeps. The reduction peak is shifted from -0.6 to -0.4, and the oxidation peak is shifted from 0.4 to 0.5 according to the data collected.

4.4 Aminophenol Gold and SPE results

Polymer particles are functionalised on electrode surface:

The voltage is specific to each polymer, which allows polymerization in a matter of seconds. Pyrrole polymerization takes around 60 s at +0.98 V. However, aminophenol polymerization takes up to 3h with the voltage of -1.3 V.

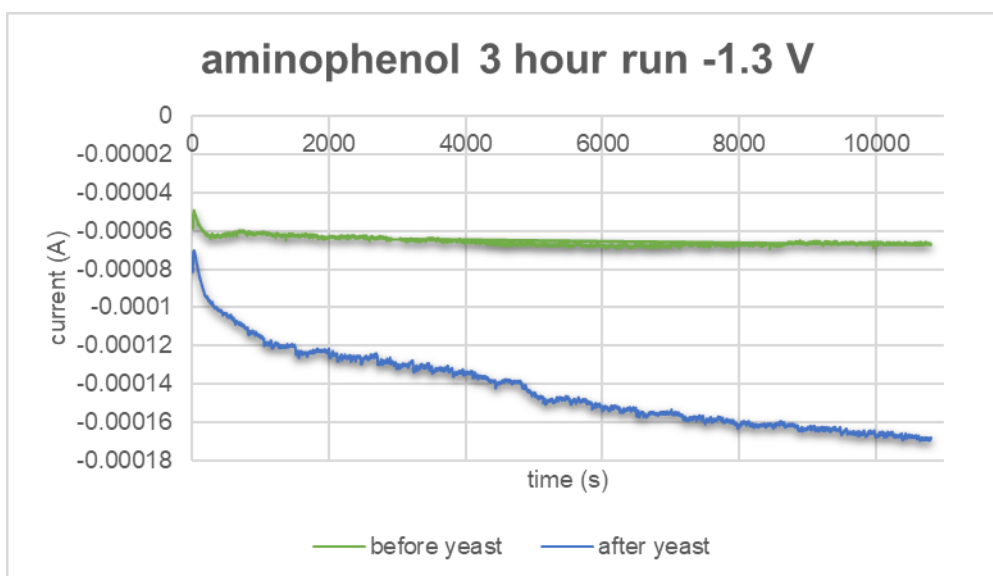


Figure 19 Graph depicting the polymerization of aminophenol MIP and NIP

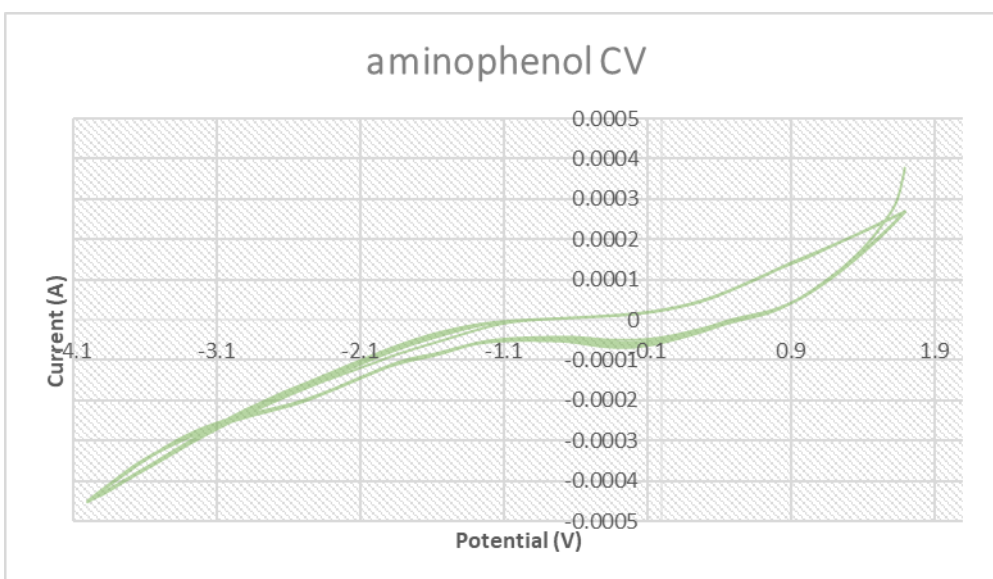


Figure 20 CV graph with two scans of aminophenol on SPE

Figure 20 is the two scan CV graph of aminophenol on SPE. Suggesting that the oxidation peak is around ranges from 0.2 to 0.3 and the reduction peak is observed in low pH values (pH 2), at around 0.5 and in a more neutral environment, around -0.1 to 0.1)

After 3 hour polymerization at voltage -1.3 CV scans of aminophenol and yeast taken using different electrodes, the last scan of all CVs are compared in the graph below:

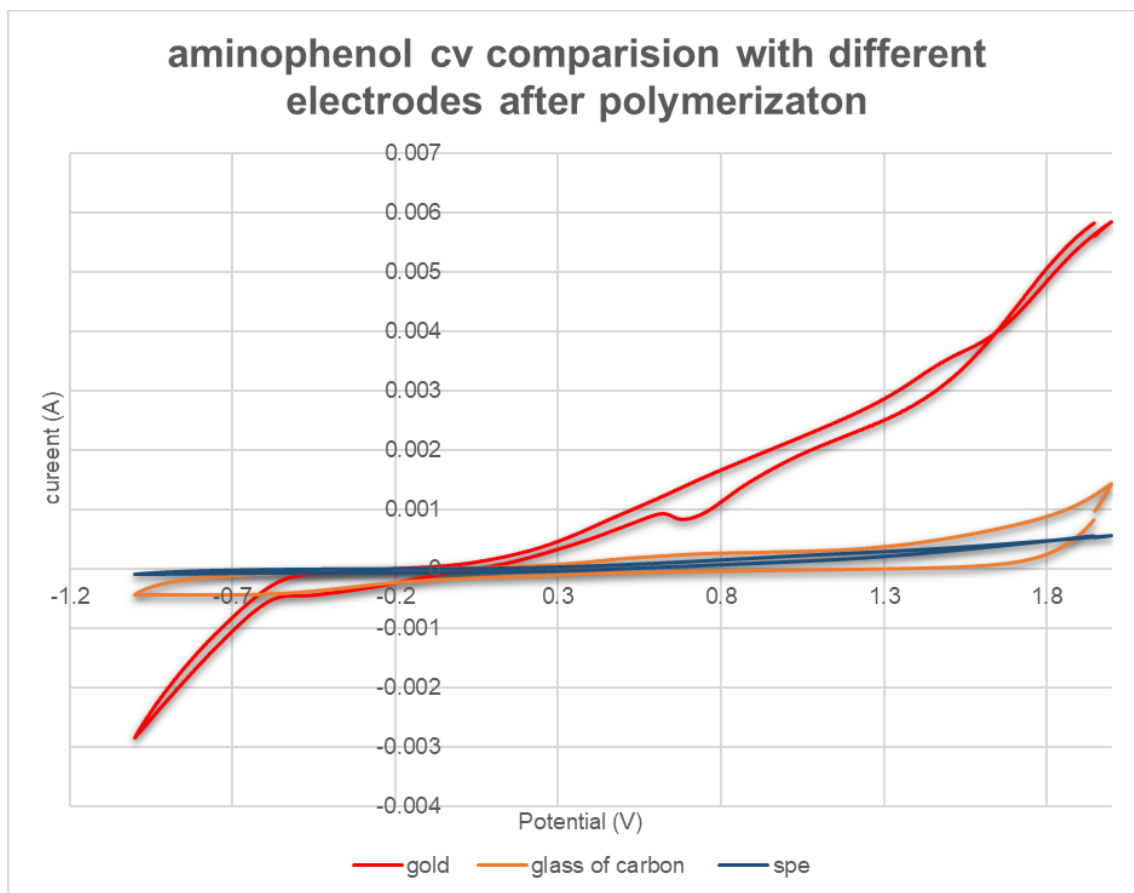


Figure 21 Graph of CV scans of aminophenol by 3 different electrodes for comparison

During the polymerization and CV scans the gold layer on the electrode was eroded due to the acidic properties of aminophenol. Correspondingly, due to the long period of polymerization and the ability for aminophenol to be able to erode gold, no further aminophenol experiments were taken place. Pyrrole was then chosen as the best monomer for the MIP and NIP synthesis.

4.5 Aluminium Electrode polymerisation results

Using aluminium electrodes and SPE electrodes pyrrole was polymerized for different durations to determine the optimum time it takes for a single layer of polypyrrole to form in PBS solution.

4.6 FTIR AI Results

Fourier Transform Infrared Spectroscopy, also known as FTIR Analysis or FTIR Spectroscopy, is an analytical technique used to identify organic, polymeric, and in some cases, inorganic materials. The FTIR Analysis method uses infrared light to scan test samples and observe chemical properties.³¹

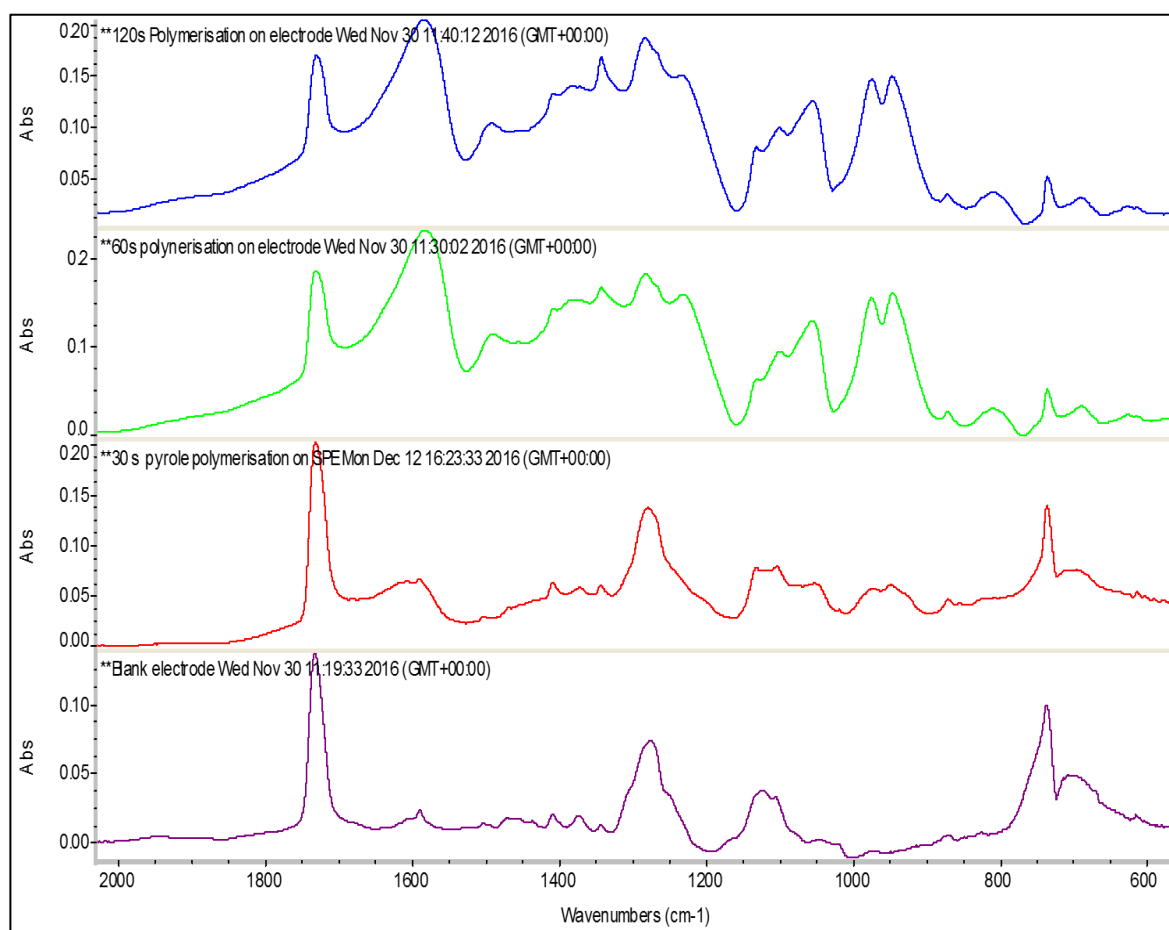


Figure 22 *IR graphs of Pyrrole on Al at different durations*

The purple graph is the aluminium electrode simply just dipped into the pyrrole and PBS solution and scanned. Suggesting that the polymerisation did not happen due to no electrochemical influence present.

The red graph shows the electrode that was polymerised for 30 seconds, the peak expected for polypyrrole (CNH at $\sim 1600\text{ cm}^{-1}$) is starting to form.

The green graph shows the electrode that was polymerised for 60 seconds and it shows the full peak has formed meaning that the shortest time needed for the polymerisation of PPY is about 60 seconds for a single layer of polymer

The blue and the last graph shows the electrode that was polymerised for 120 seconds. It shows that after 60 seconds the polymerisation has already taken place and it does not need any longer time, the longer it gets polymerised the thicker the polymer layer would be.

Graphs for 45 seconds polymerisation and 90 seconds polymerisations were also obtained but not shown here since they were similar to other spectra.

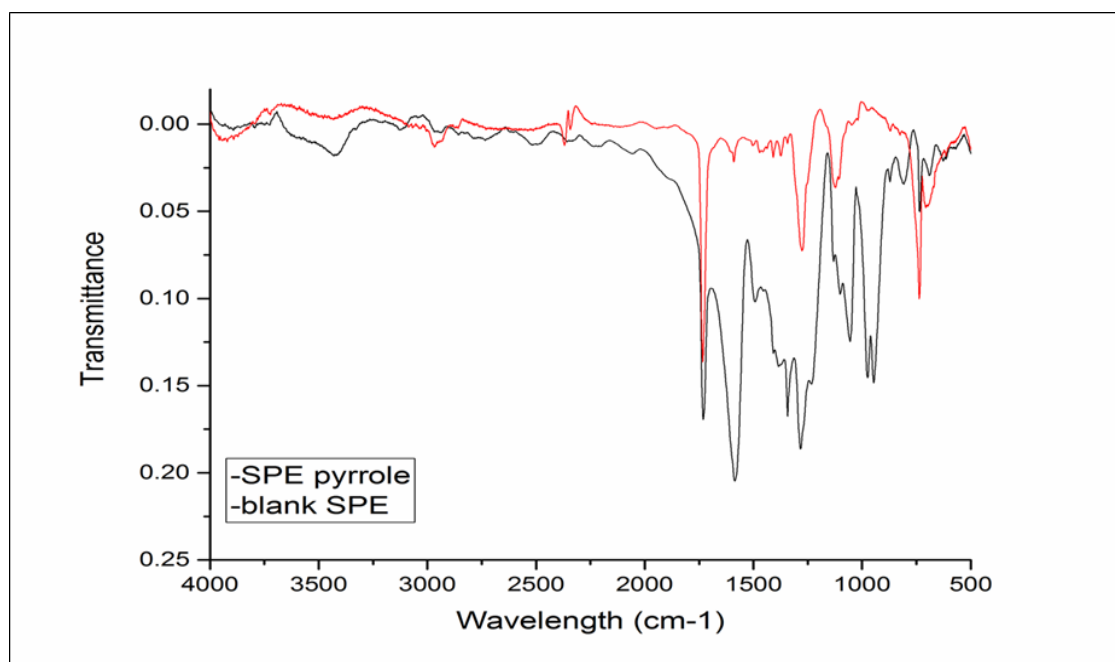


Figure 23 IR graph of Pyrrole on SPE

The peak of N-H in pyrrole is visible around 3500 cm^{-1} . There are indications of the C peaks around 300 cm^{-1} , but this signal might be distorted because of the graphite in the SPE. The graph above is to be used as a reference for the rest of the yeast HTM graphs.

4.7 White Light Scanner Results and Explanation

A white light scanner (WLS) is a device for performing surface height measurements of an object using coherence scanning interferometry (CSI) with spectrally-broadband, "white light" illumination.³² Different configurations of scanning interferometer may be used to measure macroscopic objects with surface profiles measuring in the centimetre range, to microscopic objects with surface profiles measuring in the micrometre range.

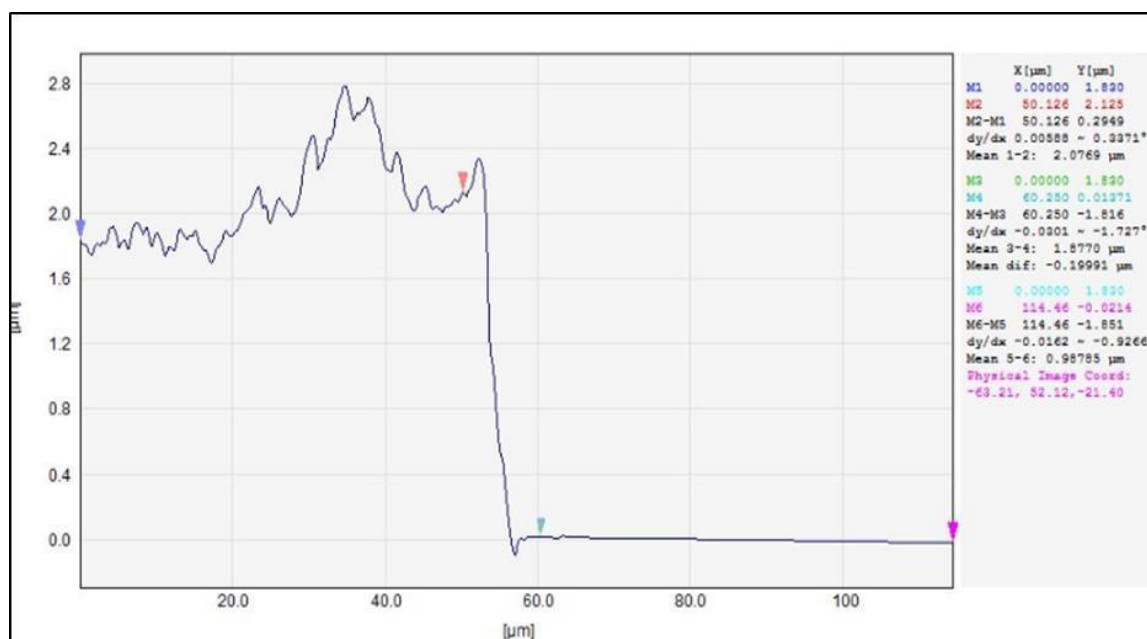


Figure 24 MIP gold graph, using the white light scanner to determine the width of the polymer layer

Using the data from the white light scanner it was determined that the average size of the MIP layer after extraction is around 4 to 7 μm , and the size of the NIP is around 2 to 4 μm .

Further pictures taken of the gold electrodes are shown below:

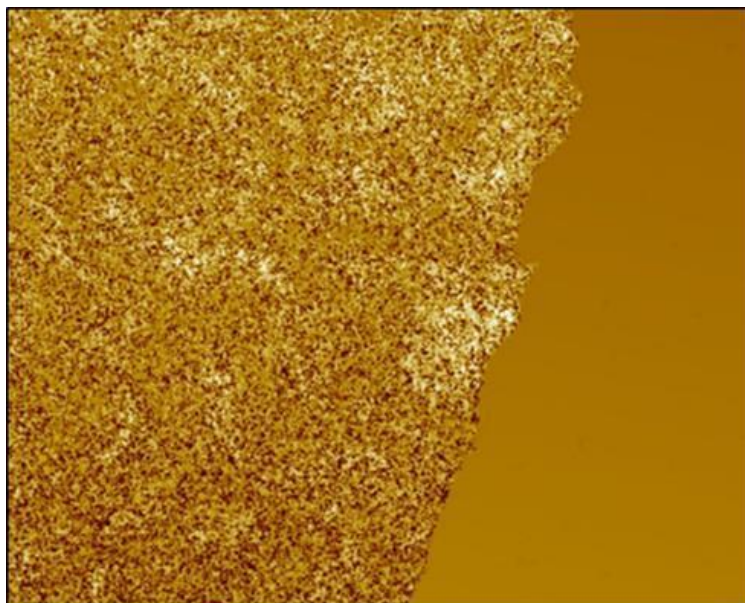


Figure 25 *MIP layer on gold after yeast extraction*

The picture taken of the gold electrode shows the MIP layer after the extraction of yeast. The smooth part of the picture is the gold of the electrode surface that was not covered in the MIP layer. The small cavities of the MIP are shown in this picture.

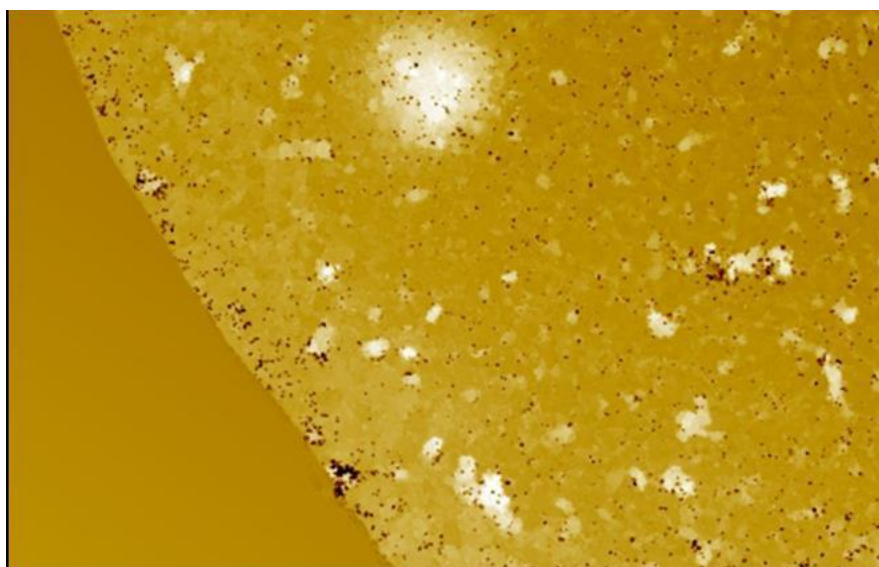


Figure 26 *NIP of yeast and pyrrole after the HTM rebinding*

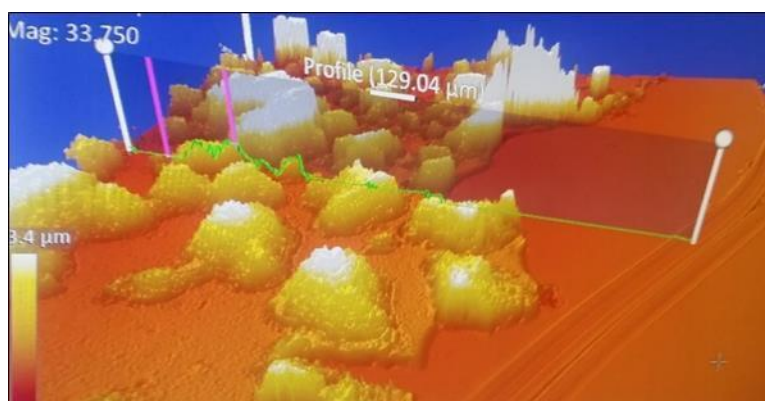


Figure 27 Yeast showing on the surface of NIP after it was used in the HTM rebinding experiment.

Both pictures 26 and 27 are of the NIP on gold electrode. The white marks on the surface are the yeast molecules that have been re-bound to the NIP after the electrode was used in the HTM experiments.

4.8 HTM SPE Graphs

A SPE functionalized with pyrrole, of which the yeast was extracted from the surface, was mounted in the thermal set up of Dr. Peeters. It was mounted onto a copper block, which was stabilized at a temperature of 37 °C. During the measurement, the sample was first stabilized in PBS and then increasing concentrations of yeast were added. The graphs shows the thermal resistance (R_{th}), which is defined as the temperature gradient between the copper and the fluid divided over the power (P). Changes at the solid-liquid interface, such as binding of yeast, have a distinct influence on the thermal resistance.

At first, the response to a blank SPE (no polymer present) was determined.

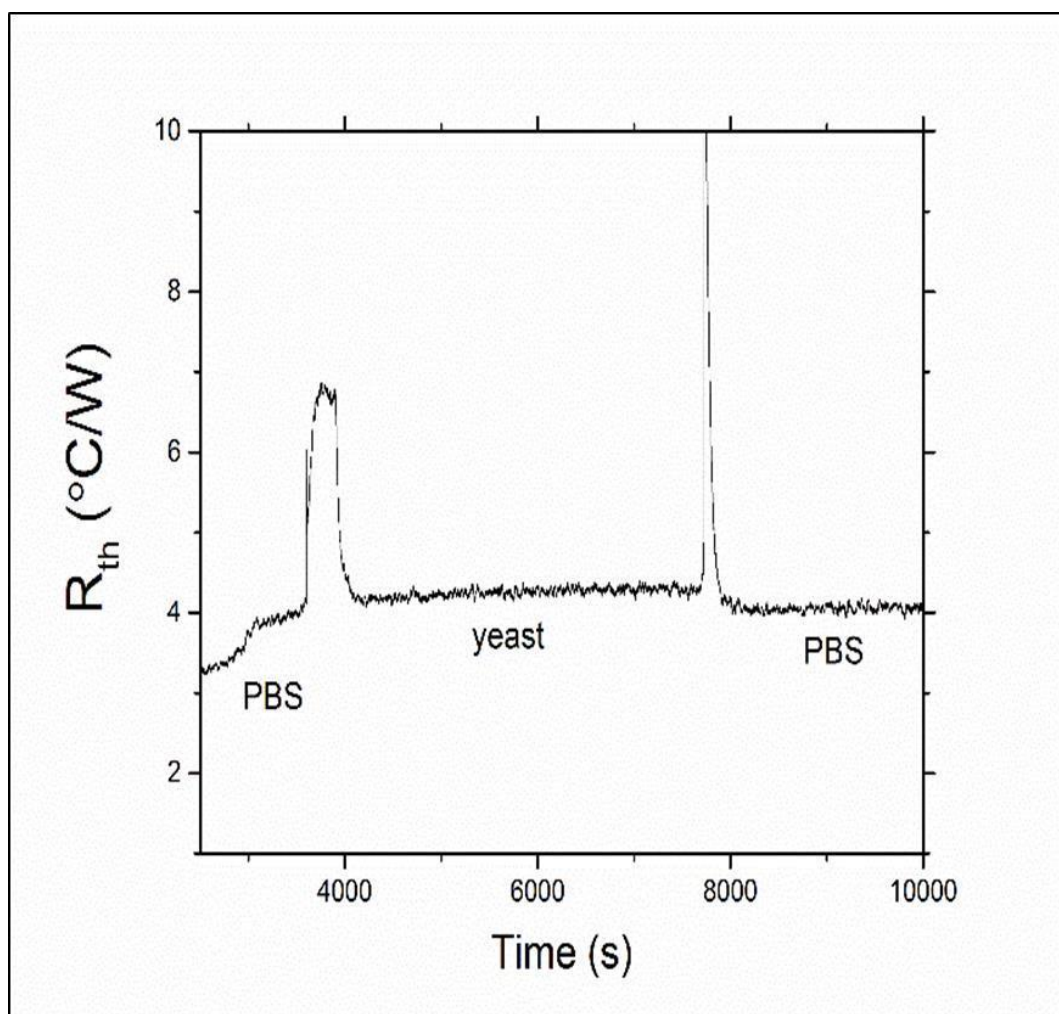


Figure 28 HTM measurement showing a blank SPE

After addition of the yeast, initially a large spike in the signal was observed. This was due to the injection of a solution at room temperature, which is significantly lower in temperature compared to the fluid in the flowcell at 35 °C. As a result, the temperature gradient is significantly higher until the PID unit corrects the temperature back to its original value. However, after a stabilization observed, the blank SPE showed no significant effect and the value returned back to baseline level (hence, no attachment of yeast to surface). This is in sharp contrast to when a polymer pyrrole layer is present on the SPEs.

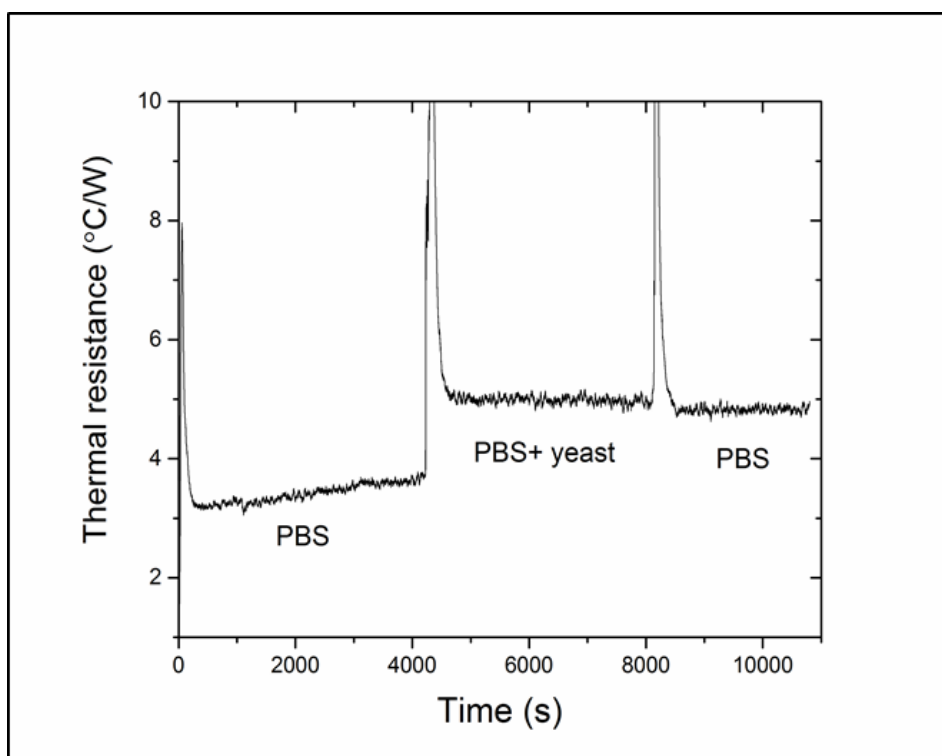


Figure 29 HTM of SPE after yeast was extracted

While there is some initial drift on the signal, it is clear that the R_{th} jumps from roughly 3.7 ± 0.1 °C/W to around 5.0 ± 0.1 °C/W, corresponding to an increase of 35% in thermal resistance. After flushing with PBS, there is only limited effect on the thermal resistance and this confirms that the yeast is firmly fixed to the MIPSPE layer.

This effect size is in line with previous experiments that were done on screening for cancer cells, where increases of up to 1.5 °C/W were recorded after cells rebound to the MIP layer. The origin of the binding of the yeast to the MIP has recently been proven by Yongabi et al.³³

Who showed with X-ray photoelectron spectroscopy and IR data that the MIP cavities contain traces of phospholipids to which the yeast are attracted. In addition, the MIP cavities are an exact fit for the size and shape of the used template molecule.

In order to quantify results, it would be necessary to construct a dose-response curve and measure the thermal signal after the addition of solutions with increasing concentrations of yeast. However, large drift signals were observed and inconsistencies in the thermal resistance values. This, in addition to the selectivity of the sensor platform, should be further studied.

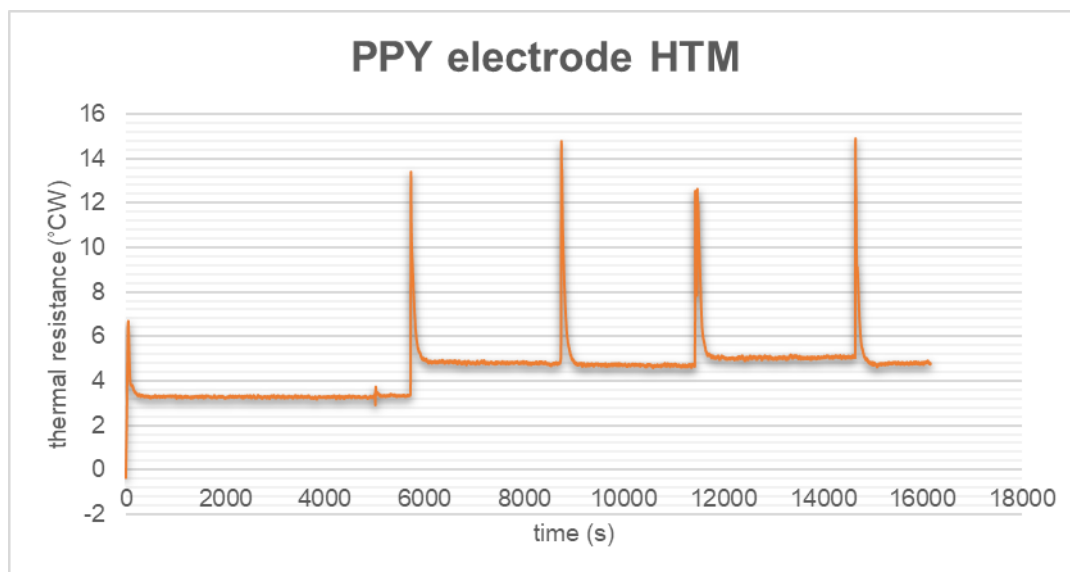


Figure 30 Dose response graph HTM of yeast SPE

The electrode was freshly prepared and extracted for a longer time. The following protocol was followed: the SPR was stabilisation for 1.5 hours, followed by 1st injection of yeast (1 ml) ,45 minutes later 2ml of PBS ,1 hour later 2nd injection of yeast (1 ml) and45 minutes later 2nd injection of PBS.

Addition of yeast led to a big response in the temperature signal (comparable to 1.5 °C). Then by flushing with PBS, yeast is firmly fixed on the surface and we only remove the outer layer (slightly lower signal). Increasing the concentration led to a slight increase in R_{th} again.

4.9 SEM images on SPEs and explanations

A scanning electron microscope uses a focused electron beam to scan a surface to create an image. The particular surface is at first plated with a monolayer of gold particles. The electrons that are present in the beam interact with the surface of the sample that produces numerous signals. These signals then can be used to obtain data about the surface topography and the composition of the sample.

An SEM is preferred here compared to an optical microscope, due to the reason that as dimensions shrink under the lenses many structures cannot be characterised by light microscopy.

The picture below shows a single layer of PPY that was polymerised onto the rough SPE surface. The graphene layer of the SPE is clearly observed to be very uneven and disordered meaning that the width and actual size of the polymer layer had to be observed on a much smoother and even surface (e.g. aluminium or gold). The powder like substance that has covered the entire image is the polypyrrole layer.

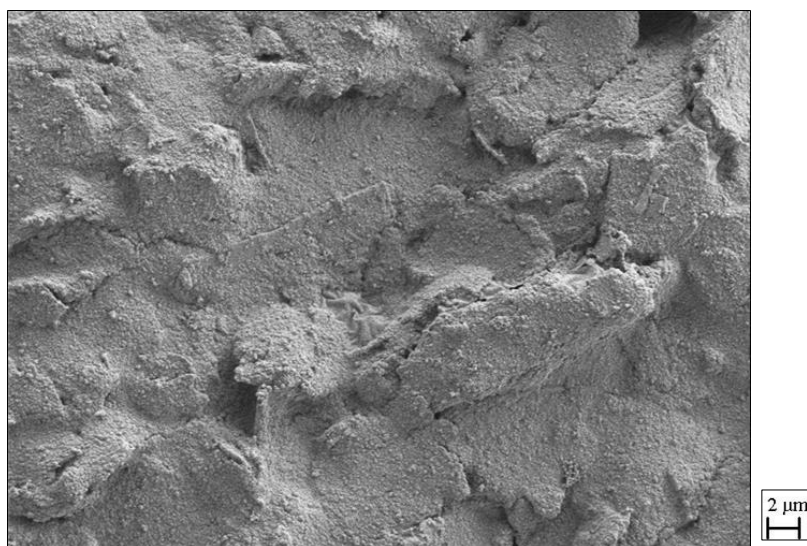


Figure 31 PPY on SPE WD =6.1mm zoom= 5K 2.00kV

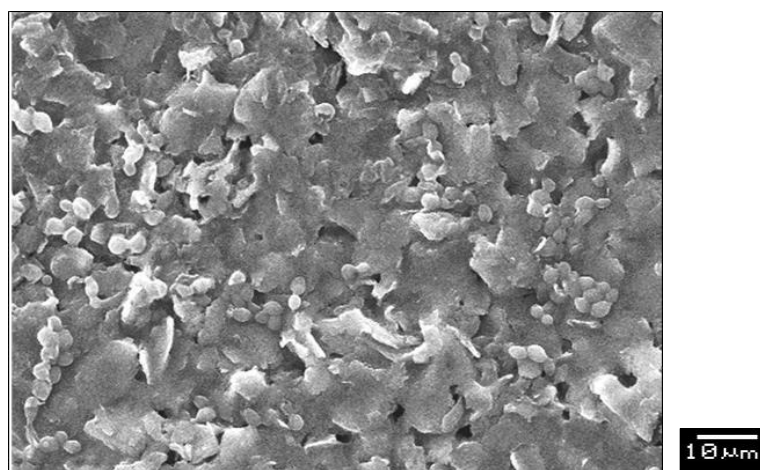


Figure 32 Yeast in PPY on SPE take with OLD SEM 20vK zoom =1000

Figure 32 is the SEM image taken of the first batch of yeast MIP synthesised on a screen printed electrode. The circular shapes observed here are the yeast molecules that have been held in place by the polymer layer. The rough surface of the SPE is likewise revealed here. The yeast cells appear to also be stuck together (perhaps this is one of the stages of mitosis as beforehand detected under the microscope when taking pictures of the yeast cells

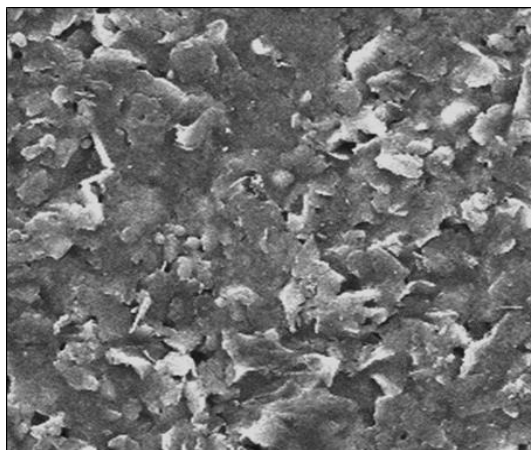
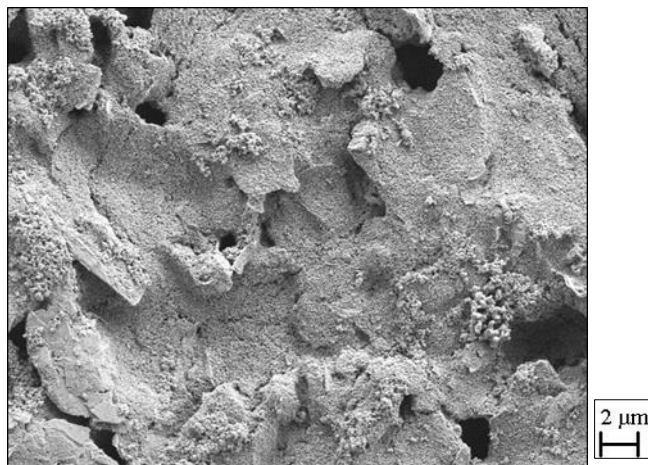


Figure 33 Taken using a different older model SEM to the other pictures

Figure 33 shows the first time attempt of extraction of yeast using hot water. The image visibly suggest that some yeast cells are still present. The small circular shapes are the yeast cells. The extraction method was repeated again and more picture using SEM were taken of the MIPs.

Figure



34 Shows the SEM image taken after the 2nd extraction of yeast

This picture shows the seconds hot water extraction of the yeast cells. The cavities that are observed are the spaces left when the year was removed resulting in the

MIP screen printed electrode. These pictures suggest that a 2nd extraction was needed for the removal of yeast.

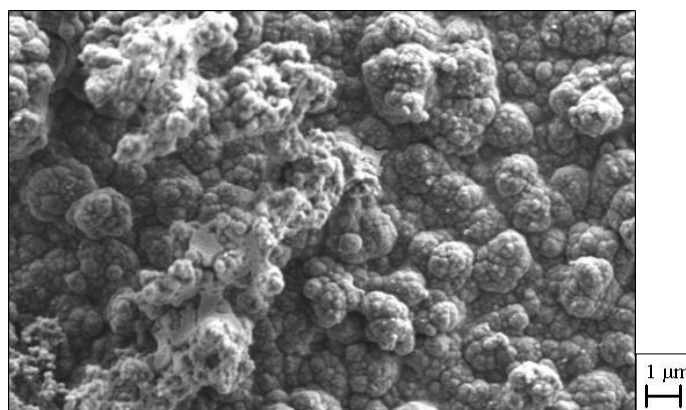


Figure 35 MIP on gold before extraction

This image is the MIP of yeast before extraction on a gold electrode the circular shapes here are the yeast molecules that appear to have been covered in a layer of the polymer, the polymer layer appears to be very thick. After polymerisation the part of the electrode that was polymerised had turned into a black colour, which was not observed on a SPE (because the graphene part of the SPEs are black).

The change in the colour is because of the redox reaction of the PPY film (pyrrole gets oxidised during polymerisation).

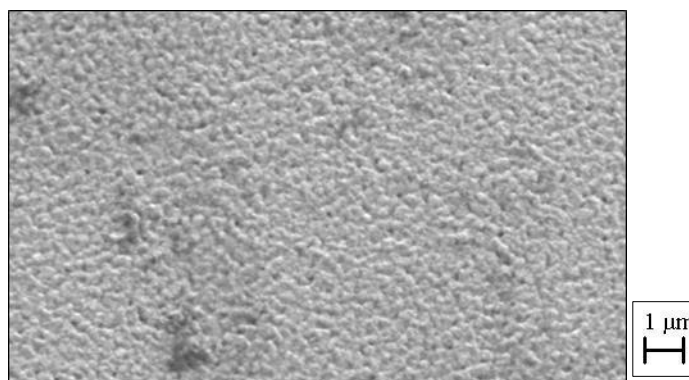


Figure 36 NIP on gold before rebinding

This image above is the image taken of the NIP monolayer on a gold electrode. The smooth even surface of the gold is shown here in this image. The NIP layer is purely a single coat of PPY.

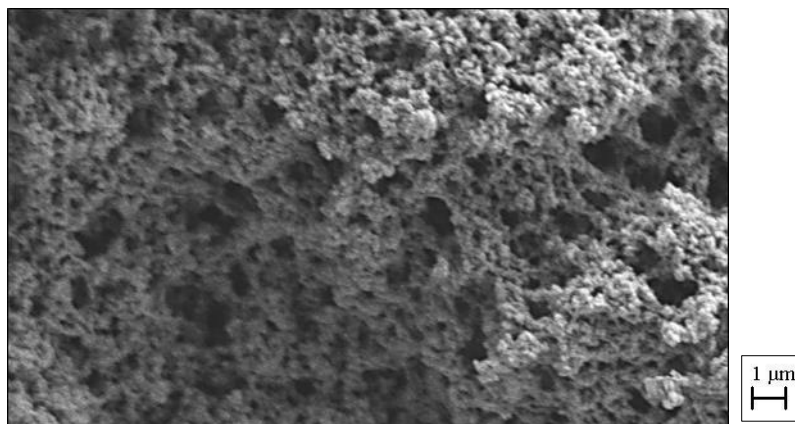


Figure 37 *Gold MIP extracted.*

The figure 37 is the picture taken of the MIP after the yeast was twice removed by being washed in hot distilled water, on a gold electrode. The cavities shown here are the holes where yeast used to be.

4.10 MRSA MIP and NIP results

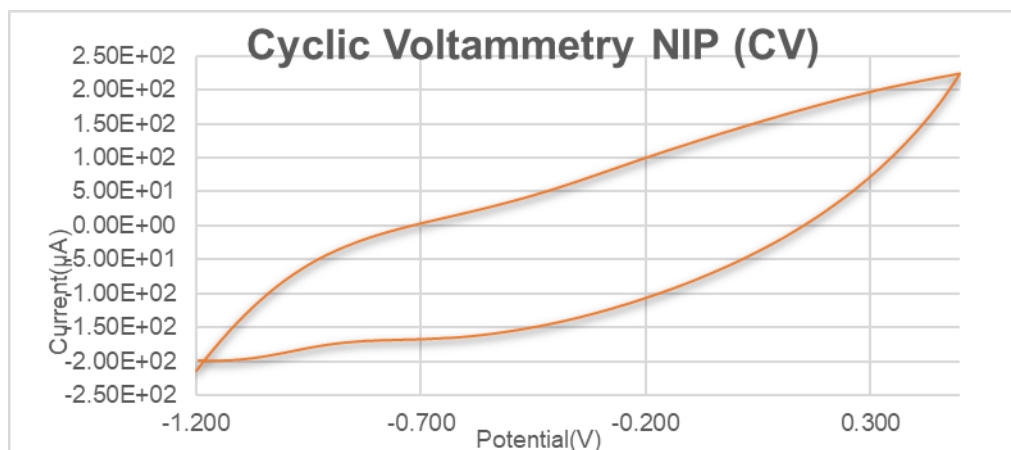


Figure 38 The graph of CV of NIP used for the MRSA experiment

Figure 38, shows the NIP SPE used for the HTM experiments of MRSA. The polymerisation took place using an Emstat. The CV in the graph shows the oxidation and reduction peaks of polypyrrole in the polymer.

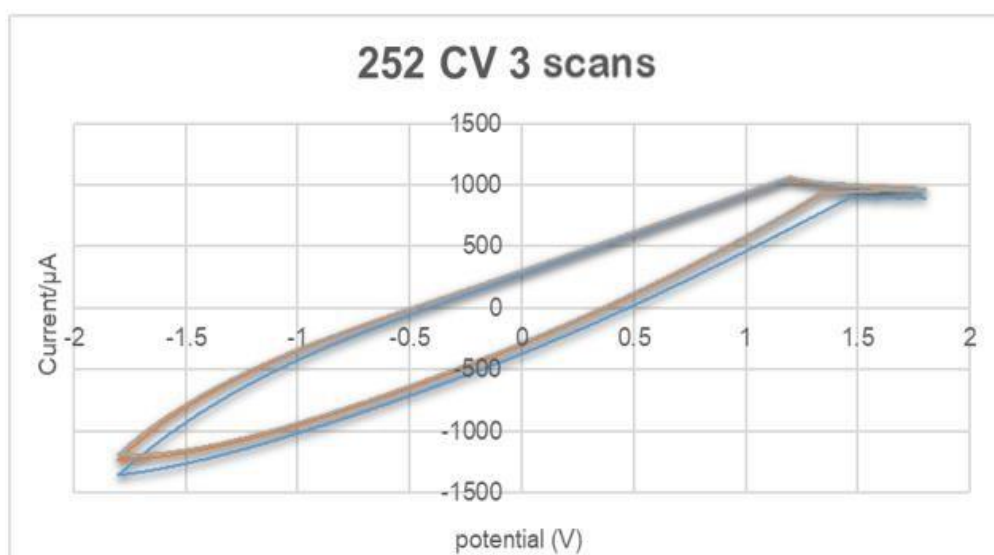


Figure 39 Graph of CV three scans of strain 252 MRSA

All three strains of the MRSA were polymerised, the graph above is the CV of the 252 strain. The MIP SPEs were cut up and 'killed off' for the HTM set up.

Each strain was used for a dose-response measurement, they were used for a 2nd dose response measurement with an injection of a different strain to check to see if the different strain would be able to bind to the MIP.

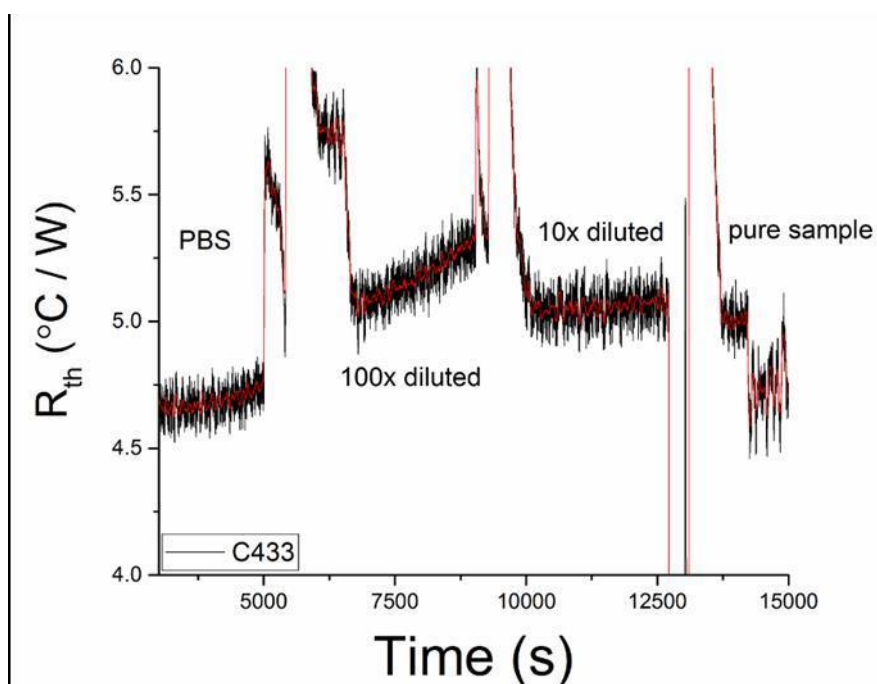


Figure 40 Graph of 3 injections of strain C433 at 37 °C

The HTM reading above initially shows that the system stabilised with PBS for about 1.5 hours, followed by the lowest concentration injection that evidently caused an increase in the signal, meaning that rebinding to the MIP takes place here. The 2nd injection is a stronger concentration to the first one, added about 1 hour later, there is slight increase compare to the stabilised line, however the graph appears to be stabilising again. The thurst injection is the pure sample (strain C433)

being added last does not cause an increase meaning that the cavities on the surface of the MIP are fully saturated at this time.

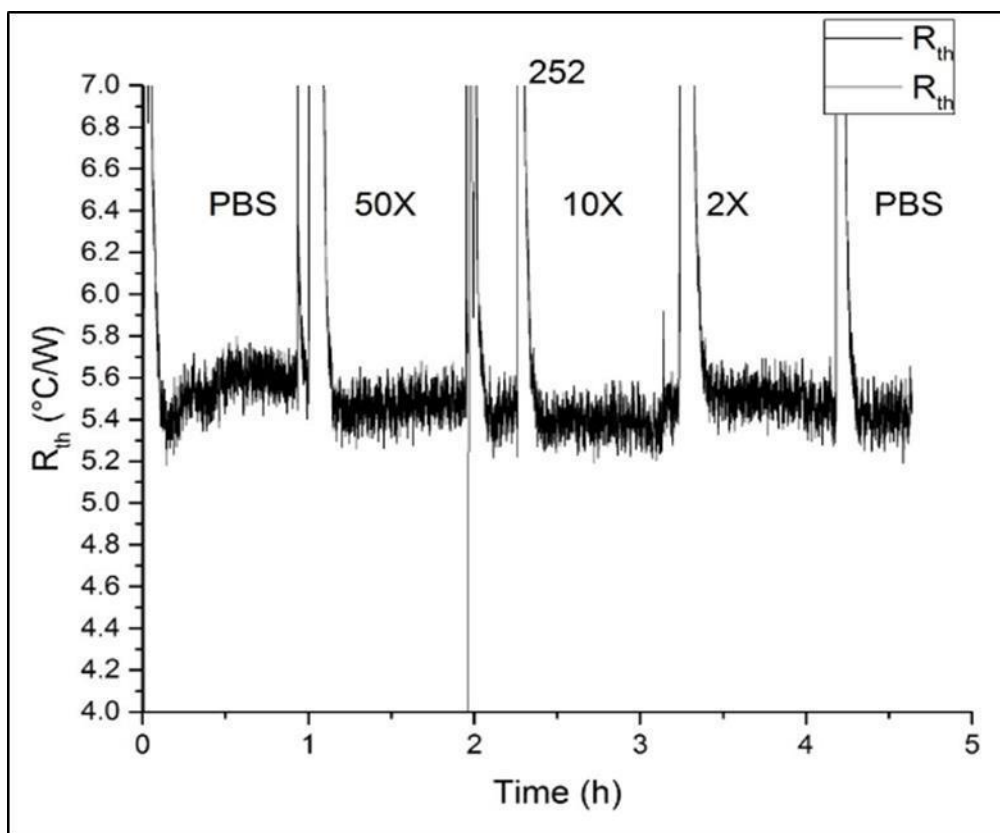


Figure 41 Dose response graph of strain 252 at 37 °C

This graph shows the dose response reading of strain 252. The extracted MIP was first stabilised with PBS, however, the curve shows that it was not fully stabilised. Followed three injections of different concentrations of the same MRSA strain, *(each injection was followed by a small injection of PBS to wash the MIP)*, then a PBS final injection was added to as an attempt to wash off the MIP and stabilise the reading.

Each injection of the MRSA caused a slight initial increase in the readings, this was due to the cells re-binding to the surface of the MIP where its receptor cavities were.

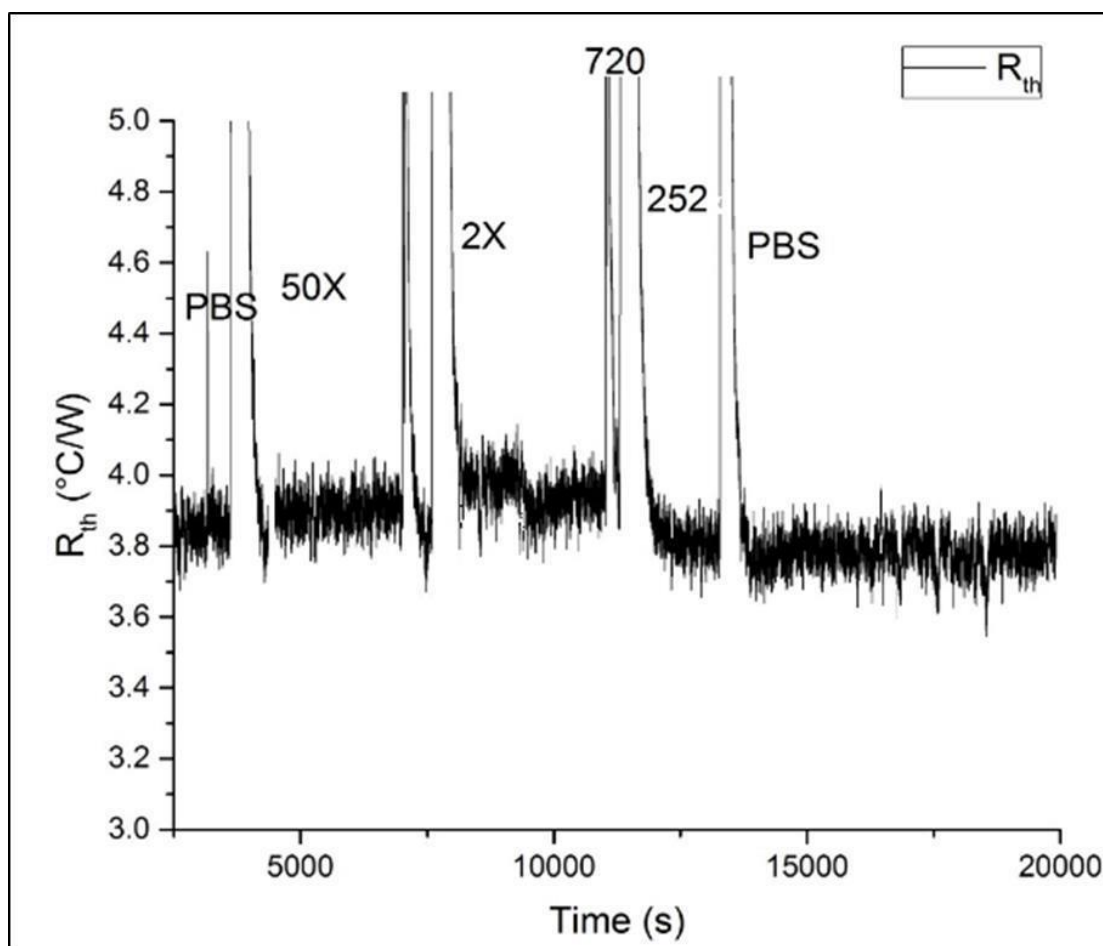


Figure 42 Dose response graph of MRSA strain 720 at 37 °C

This graph shows that the extracted MIP was stabilised in PBS, followed by increasing injections of the same strain, that show a minor raise in the signal suggesting the re uptake of the strain by the MIP. The 2nd injections of 720 shows a bigger raise in the signal because, it has a higher concentration, however after about 45 mins, it is observed that the graph goes steady again, this could suggest that the MIP is now saturated. The system is washed with PBS and an injection of strain 252 is added to the flowcell that starts to decrease the signal, this could mean that the 252 cells are not binding to the 720MIP, the system is then stabilised again with a high dose of PBS and it does appear to go steady.

4.11 MRSA and E. coli Microscope Pictures after Staining

These pictures of the MRSA and E. coli were taken using the staining process explained before and light microscope. In some pictures it is difficult to determine if the picture is showing a gram negative or gram positive bacteria. This is due to the fact that a very thick smear diminishes the volume of light that can pass through, consequently, making it difficult to visualize the morphology of single cells. Smears normally require only a minor quantity of bacterial culture.

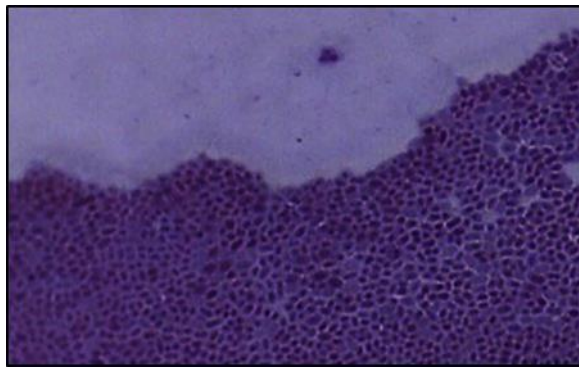


Figure 43 MRSA 252 strain

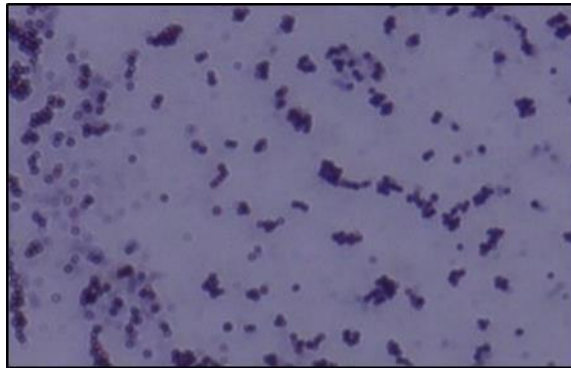


Figure 44 MRSA strain 252 2nd attempt at staining

Figure 44 shows the right amount of smear needed for a picture of the MRSA, compared to figure 43 (*where the smear was too big and it was not clear what exact colour the MRSA was*). The MRSA pictures show a dark purple colour suggesting that the strains are gram positive bacteria.

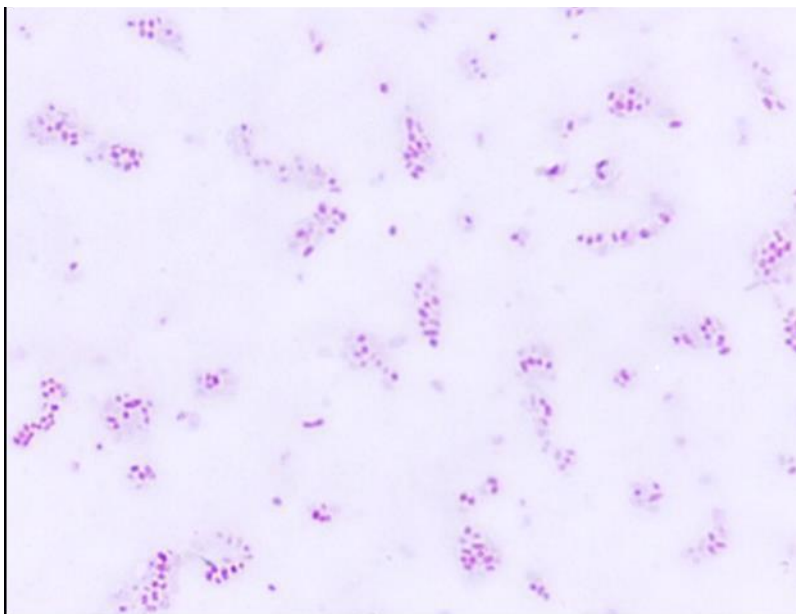


Figure 45 *E. coli* picture under the light microscope strain 10215

The picture above is the picture taken of the *E. coli* strain 10215 after staining. It shows a pink colour suggesting that *E. coli* is a gram-negative type of bacteria.

4.12 Yeast Gold HTM Results

All of the yeast experiments were repeated using the gold electrodes using the same protocol as it was used for the SPEs

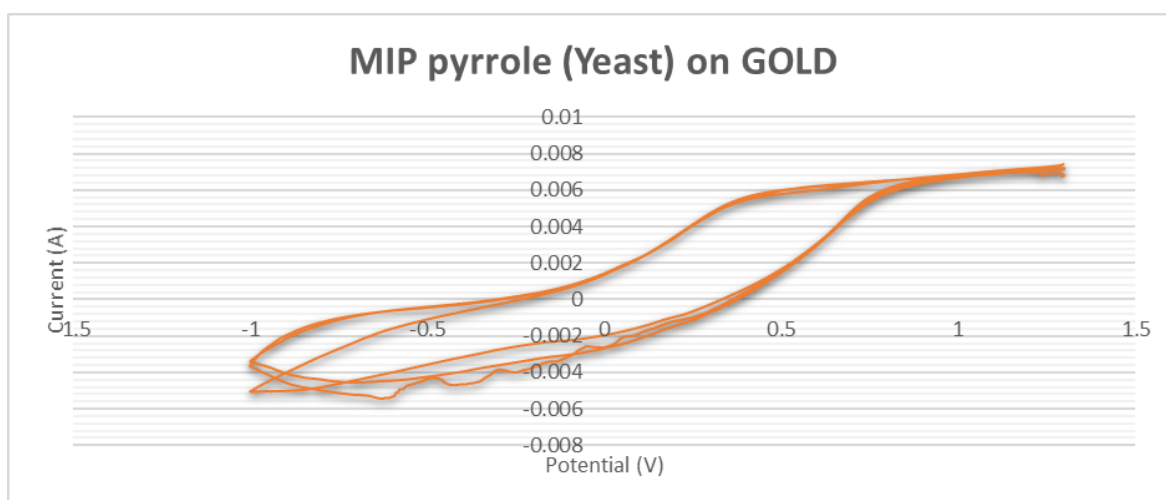


Figure 46 CV of yeast PPY MIP on gold electrode three scans

The CV scan shows three sweeps of the yeast MIP on the gold electrode, the first 2 scans show the oxidation peaks and reduction peaks clearly with a slight shift due to the presence of yeast, but the 3rd scan appears to have lost signal towards the end of the reading. The loss of signal was due to the reference electrode moving and unclipping from the sensor at the very end. The experiment was then repeated to obtain a better graph.

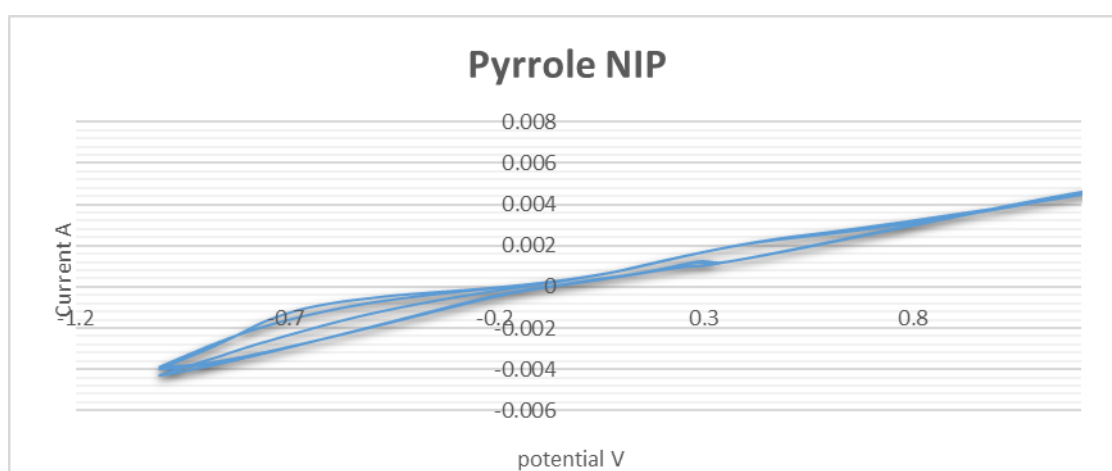


Figure 47 Graph of NIP gold electrode

Figure 35, shows that nip layer on the gold electrode showing the peaks of polypyrrole as expected.

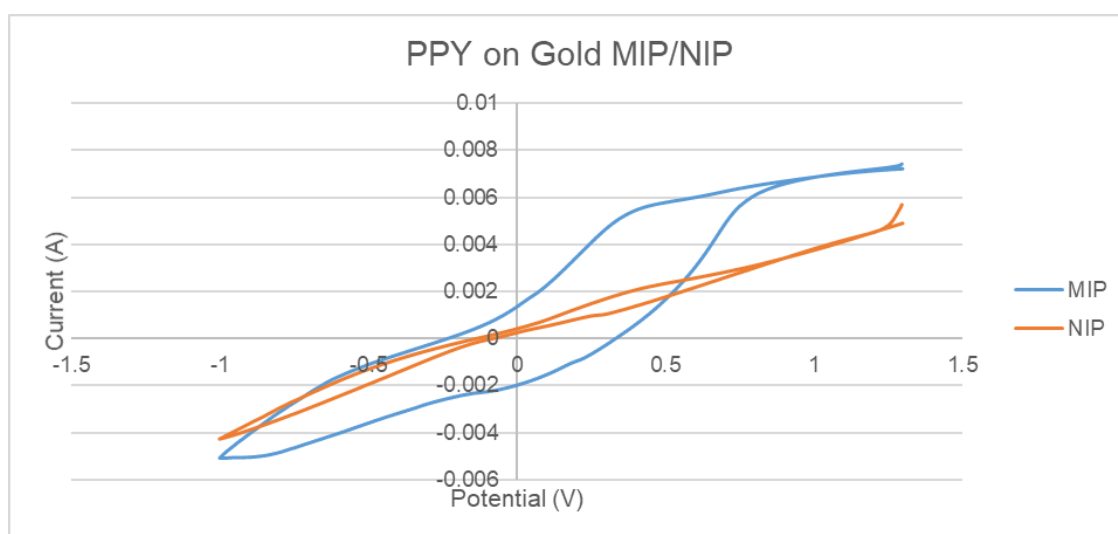


Figure 48 Graph comparing CV of NIP and CV of MIP of gold electrodes with yeast

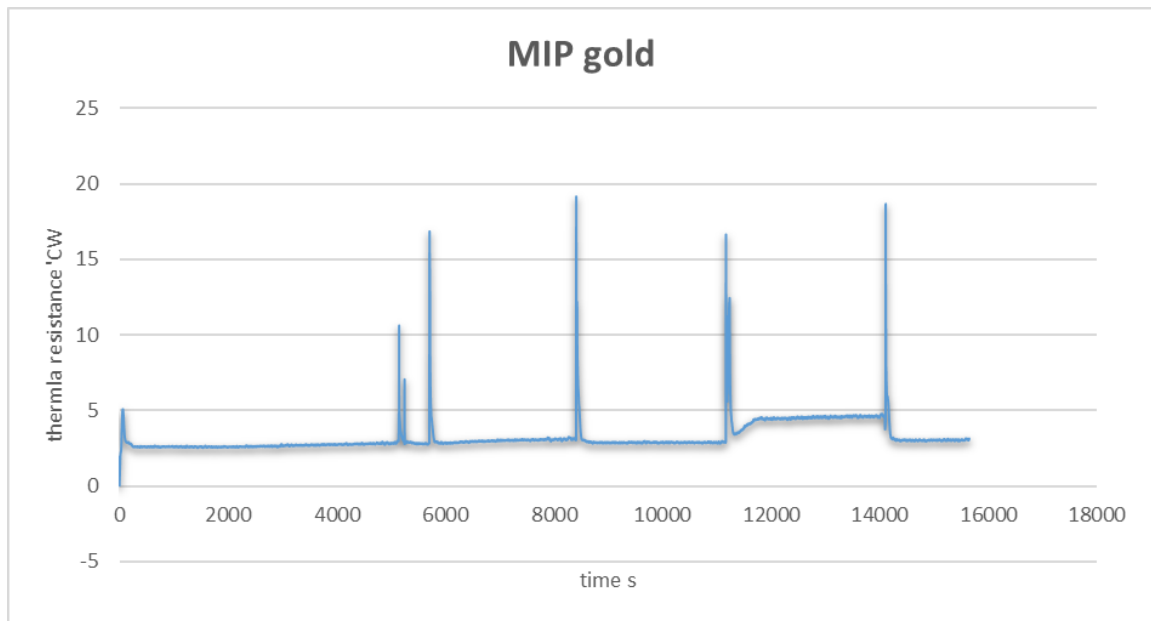


Figure 49 HTM reading of yeast on gold MIP electrode

The MIP gold electrode was stabilised for 1.5 hour with PBS, followed by three injections of increasing yeast concentration, then finally it was washed with PBS again and left to stabilise. The R_{th} value after each injection suggests that the yeast was re binding to the MIP.

The R_{th} value is calculates using excel via the following formula:

$$R_{th} = \frac{(T_1 - T_2)}{P}$$

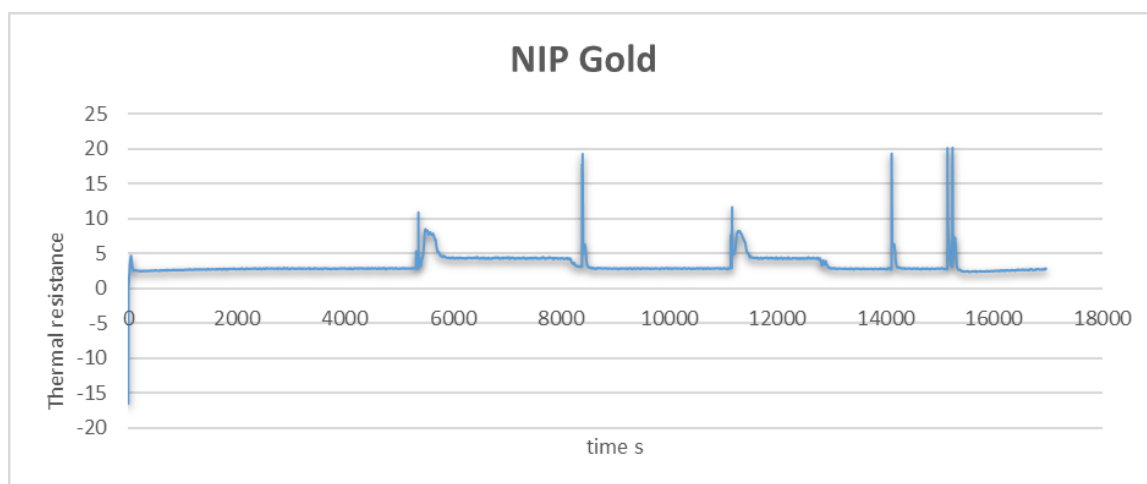


Figure 50 NIP gold electrode after HTM

The HTM graph of NIP followed the same procedure as the MIP, showing a small rise in the signal initially meaning that the yeast is binding to the surface, but the signal does drop suggesting that the NIP has been saturated with the template.

4.13 Bulk Polymerisation Tables and Graphs of Results

The protocol explains before was used to synthesise bulk (powder) polymers for yeast using pyrrole as its functional monomer. The MIPs were dark brown colour and the NIPs were a white creamy colour. After a few attempts of filtering off the yeast it appeared that the yeast was too big to grow though the filters attached to the syringe, the batch rebinding dilutions were then filtered off using filter paper however, the yeast were too big to be filtered off again according to the absorbance data that was collected again. A graph comparing the MIP and NIP absorbance of yeast is shown below.

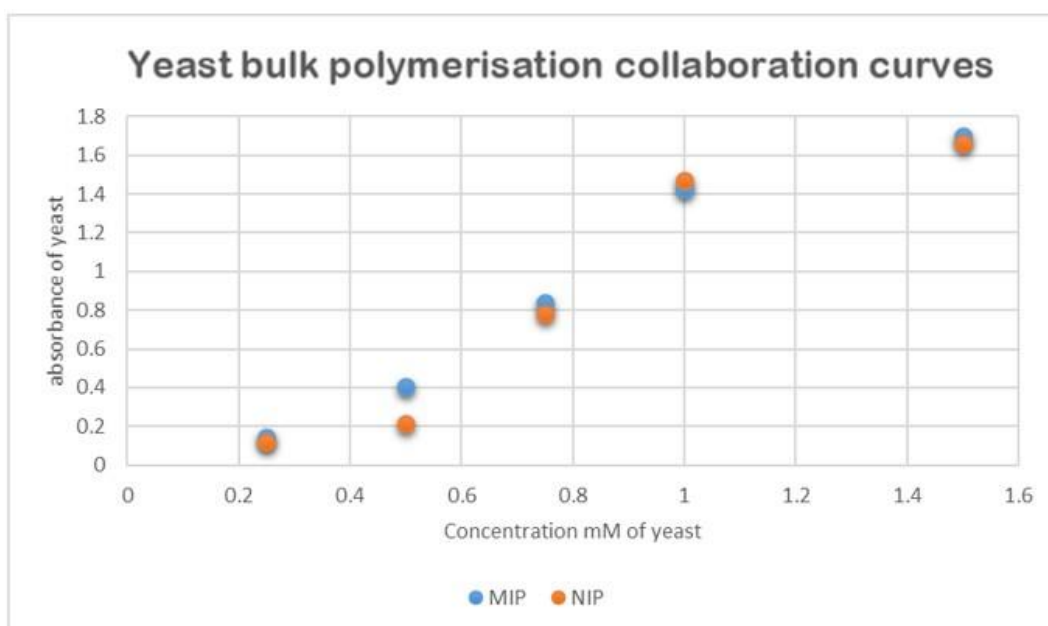


Figure 51 Yeast bulk polymerisation showing absorbance of MIP and NIP before rebinding.

The table below shows the concentrations of yeast used for the preparation of the UV-VIS with the amount of MIP and NIP that were added to each vial, which were the shaken on the orbital shaker for 3 hours before the attempt to filter them.

Yeast absorbance before batch rebinding				
Yeast Concentrations (ml)	MIP absorbance at 640 nm	MIP Pyrrole (mg)	NIP absorbance at 640 nm	NIP Pyrrole (mg)
0.25	0.145	8.5	0.177	8.5
0.5	0.403	8.6	0.213	8.5
0.75	0.841	8.5	0.782	8.4
1	1.424	8.5	1.47	8.6
1.5	1.698	8.5	1.66	8.5

The MIP and NIP for yeast were synthesised using MAA as the functional monomer instead of pyrrole. Unfortunately, the filtration of the new polymers also failed.

Refer to the appendix for the IR data regarding the bulk NIP and MIPs

4.13.1 Bulk polymerization of antibiotics

A typical example of a batch rebinding experiment is given in Figure 52. To quantify how much of the template bonded to the polymer, polymer and citrate buffered solutions with a known concentration of Amoxicillin were mixed for 12h (this was determined to be optimal binding time). These suspensions were then filtered, and it was measured how much amoxicillin was left in the solution, which enabled to quantify how much had bound to the polymer. A typical example of what we call a batch rebinding curve is given below, demonstrating there is a difference in the amount of template bound to the MIP vs to the reference NIP (Fig 13).³⁰ *The preparation of the NIP and MIP of the antibiotic was carried out by me demonstrating to Jessica Pimlott, batch rebinding was done completely by her. Jessica has given me permission to use the data to contrast the following graph.*

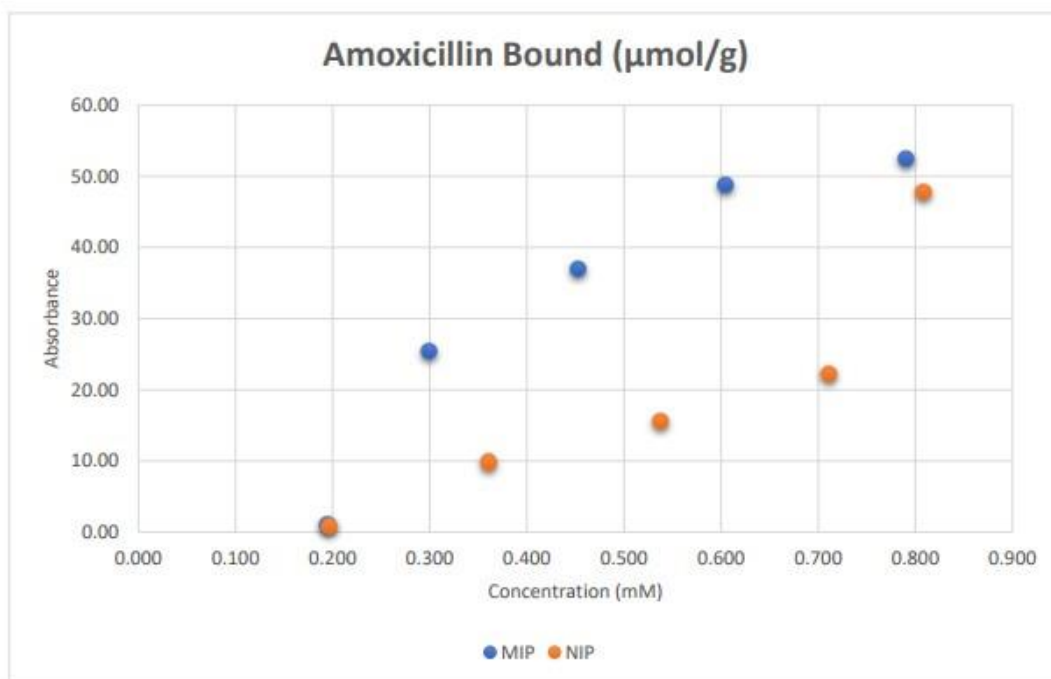


Figure 52 MIP and NIP batch rebinding of amoxicillin

A typical batch rebinding curve, demonstrating the difference between the MIP and the reference polymer.

This experiment was later on repeated three and similar results were obtained, demonstrating reproducibility of the method.

4.14 E. coli MIP and NIP results via the HTM

The two strains of E. coli were used to make MIP and NIP screen printed electrodes using the Emstat. Screen printed electrodes were used as the reference and counter electrode in these experiments.

Each MIP was used for a dose response graph and an additional MIP was made for the 2nd dose response graph with the injection of the different strain.

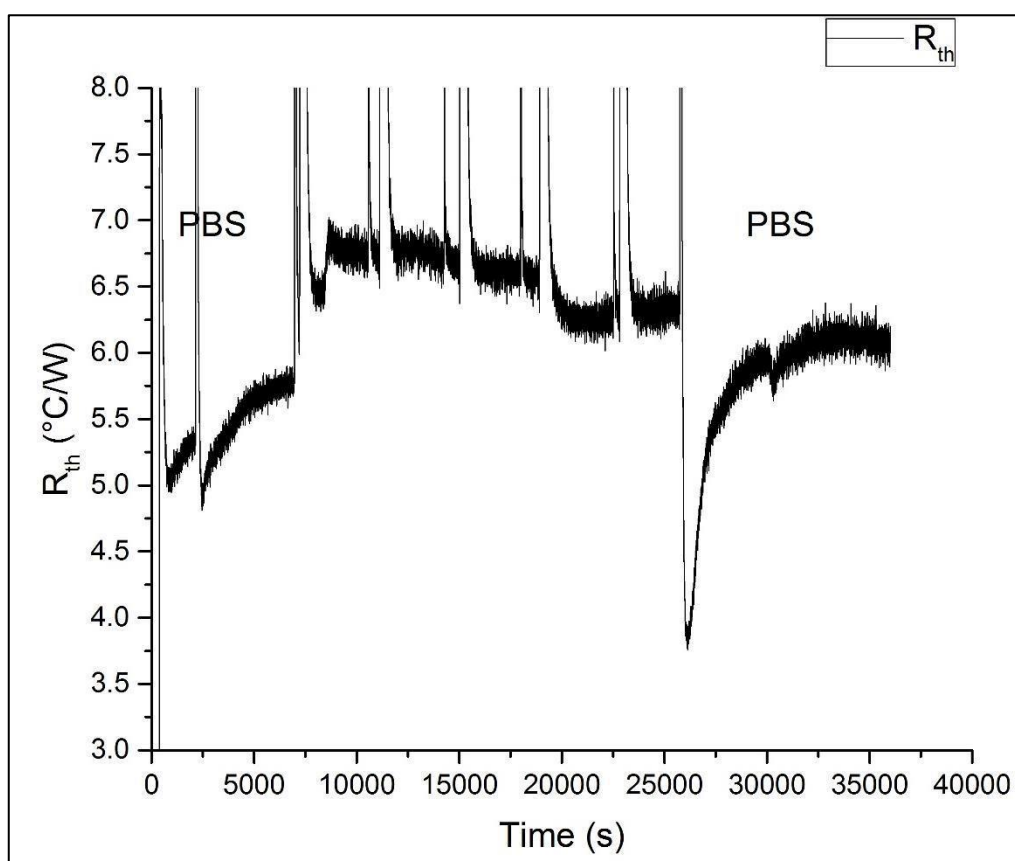


Figure 53 Graph of dose response 10215 PBS stabilisation E. coli strain 1

This graph shows that the MIP was first stabilised with PBS, when the four increasing concentrations were added the signal appeared to be risen higher than the stabilisation point suggesting the re binding of the bacteria strain and it slightly decreases with each injection meaning that perhaps with each injection there is less surface area for the bacteria cells to bind to.

The injected added second to last is strain 23849, it shows that the MIP does not re bind to the different strain the signal appears to be steady, and this could also suggest that the MIP is fully saturated at this point.

The final injection is PBS to wash off the MP and re-stabilisation appears to happen sometime after that final injection.

The second signal that appears after each injection is when the flowcell is injected with a small amount of PBS to wash the tubes to avoid back flow of the previous injections. It was also a method to wash off the 'adhesive' bacteria from the tubes.

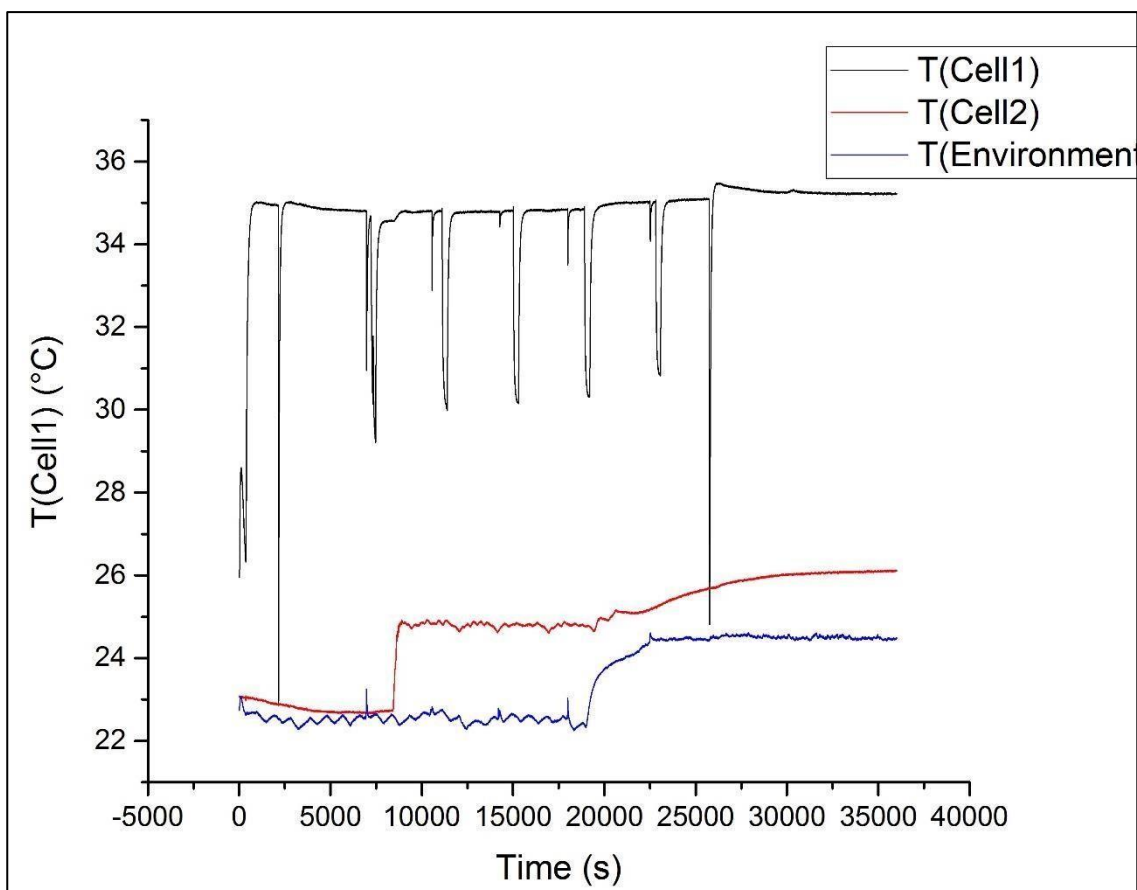


Figure 54 HTM graph of 23849 dose response

Figure 54 shows the HTM graph of 23849 dose response. The difference in signal around 20.000 s is caused by the turnoff of the AC unit, influencing the environment and incubator temp, as is seen in the graph, the black line is inside the flow cell, and the red line is the incubator temperature, while the blue line represents the temperature outside the incubator.

4.15 NMR data of pyrrole

NMR data of pyrrole were obtained to compare to the other analysis to see where the peaks of pyrrole appear.

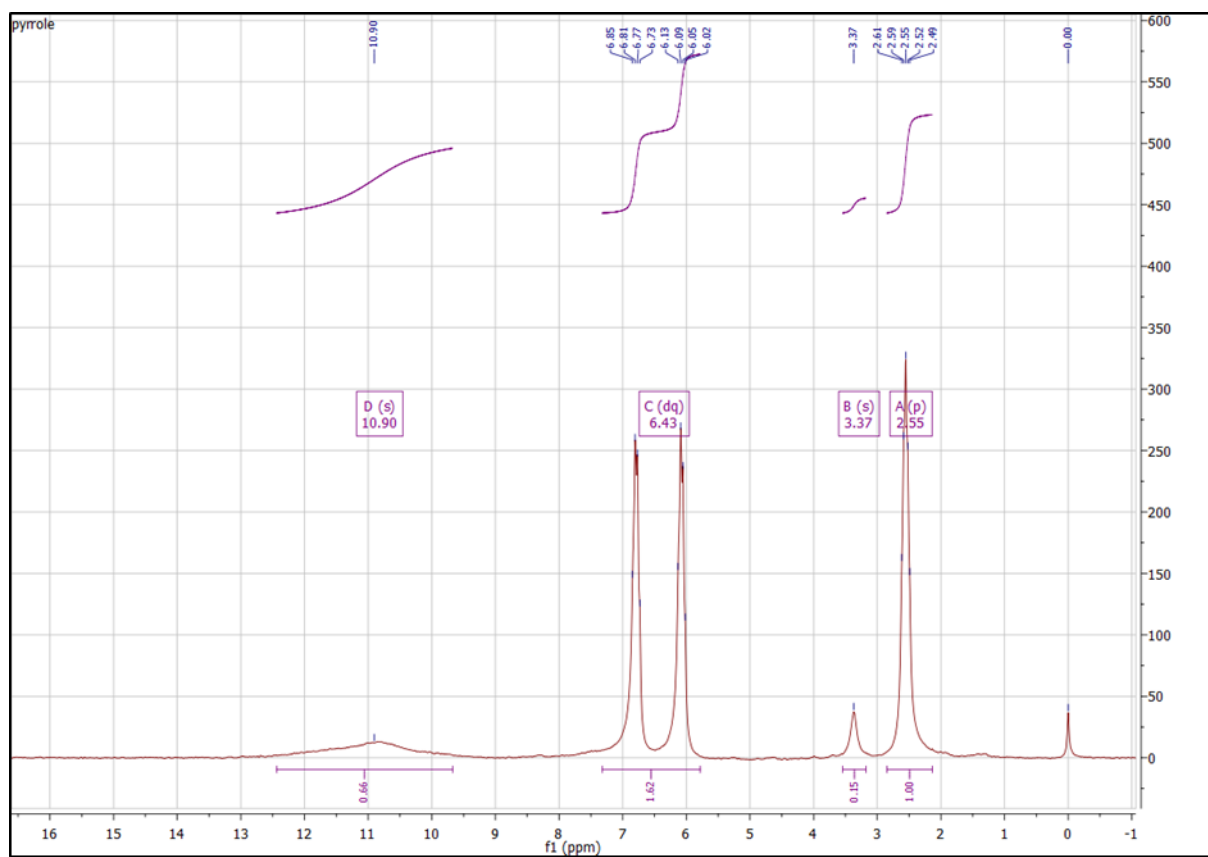


Figure 55 Low field NMR of pyrrole

5. Conclusions

The aim of this work was to develop MIP-based sensor platforms for the thermal detection of micro-organisms. In first instance, MIPs for yeast were developed using electropolymerisation. Pyrrole and aminophenol were mixed with yeast and deposited onto a range of electrodes, including SPEs, gold and aluminium. Subsequently, extraction was performed with various media to remove yeast from the surface and to obtain micron-sized nanocavities that are an exact fit for the size and shape of the template molecule. SEM images showed that two extractions with hot water were required to remove all yeast from the surface. It was attempted to visualize the micron-sized cavities that are present on the surface of the electrode, but this was complicated due the roughness of the SPE electrodes. In addition, there is little contrast between the peaks of the polymer and the graphite-based ink, which made it not possible to monitor the polymerization process with IR or measure the thickness with SEM.

Gold electrodes, which a much smoother surface, were in that sense a better alternative. It was determined by monitoring the N-H peak in the IR spectra that the optimal polymerization time was 60 s. Furthermore, by covering part of the surface and measuring the step height with white light profilometry, it was possible to estimate the thickness of the MIP layer and confirm the presence of cavities on the surface.

However, SPEs have distinct advantages over the metals such as high reproducibility and low-cost. Therefore, it was decided to use those electrodes for thermal detection experiments with yeast. In an initial study, it was observed that a sharp increase in the thermal resistance was observed after addition of yeast to the MIP. This was in contrast to the reference measurements, where no significant

response in the thermal signal was seen. It was a first proof-of-application of the MIP-based electrodes for the thermal sensing of yeast, and therefore it was decided to move towards *E. coli*, a pathogenic bacteria.

Imprints were prepared by electropolymerising pyrrole in the presence of *E. coli* and removal of the bacteria with hot water. These MIP-functionalized SPEs were mounted into the thermal set up and the response to different concentrations of dead *E. coli* solutions were monitored. Some signals did suggest that the rebinding was taking place but, no conclusive results were obtained due to large drifts in the signal. In addition, it could be that no significant response was observed because the *E. coli* cells were no longer alive, which is because otherwise it would not have been possible to handle them on the 7th floor labs. Towards the end of this research, when the *E. coli* experiments were taking place, the HTM set up was malfunctioning due to the small thermal connections sometimes the system was not able to keep the temperature at same for the experiment that led to many errors in the signals and many of the data had to be repeated. However, the HTM experiments for the MRSA cells did prove to be more successful according to the results that were discussed.

In summary, the preparation of MIP-functionalised electrodes with electropolymerisation is a promising technique because it allows to control the polymerization process and obtain nanosized surface architectures. A first proof of application for the sensor was provided with yeast, but further research would need to be conducted in able to construct calibration curves and quantify the amount of target present. MIPs are versatile and can be adapted to its application, meaning this gives potential to develop an array where we can monitor various biomolecules at the same time. This could lead to the development of a bacterial

fingerprint, or potentially monitoring antibiotics at the same time as bacteria which could provide insight into how microorganism develop antimicrobial resistant properties.

6. Future Work

The use of HTM shows promise for the detection of bacteria. However, there were issues with the stability of the measurements during the course of this project. This is partly due to continuous improvements of this home-made set up, and technical issues that were encountered. More measurements should be performed to construct dose-response curves for yeast and MRSA to quantify the results. In addition, selectivity could be further evaluated by studying the response of the electrodes to similar strains of bacteria.

The use of MIP-SPEs is compatible with other detection methods, such as cyclic voltammetry or optical detection methods. Benchmarking of the thermal detection method is necessary to add value to the results obtained within the project. The design of the used flowcell could be adjusted to adopt an array format, which will allow to simultaneously monitor a range of molecules and determine bacterial fingerprints. To demonstrate proof-of-application, we should move to relevant food samples or evaluate the limit of detection in clinical samples.

7. Acknowledgments

I would like to specifically thank my supervisor Dr M. Peeters for all her help and time she spent training. In addition, I would like to thank Kai Betlem for his help with the HTM set up and his supervision in the labs throughout my study, and Jessica Pimlott for her contribution in the collection data for the antibiotic experiments. I would also like to thank the microbiology team including, Prof Mark Enright, Dr Misha Zubko and Elliot Whitetard. Finally thanks to Dr. Chris Liauw for the FTIR and WLS training and a thank you to Craig Banks for his resources.

8. Notes and References

1. G. Vasapollo, R. Sole, L. Mergola, M. Lazzoi, A. Scardino, S. Scorrano and G. Mele, *Int. J. Mol. Sci.* 2011, **12**, 5908-5945.
2. P. Sharma, A. Pietrzyk-Le, F. D'Souza and W. Kutner, *Ana. Bio. Chem.* 2012, **402**, 3177-3204.
3. F. Trotta, M. Biasizzo and F. Caldera, *Mem.* 2012, **2**, 440-477.
4. R. Suedee, *Pharm Anal. Acta.* 2013, **08**, 04.
5. M. Babu, *Bact. Gen. Reg. Trans. Net.* Caister Academic Press, Norfolk, 2013, **9**, 139.
6. Y. Tor, R. Fair, *Perspectives in Medicinal Chemistry*, Zoe Kruze, Oxford, 2014.
7. T. Thompson, T. Stephens, G. Loneragan, M. Miller and M. Brasherars, *J. Food. Protec.* 2007, **70**, 2230-2234.
8. W. Hagmann, *An. Rep. med. Chem.* Academic Press, San Diego, 1993.
9. *Global Public Health*, 2007, **2**, 103-106.
- 10.3.K. Jayalakshmi, M. Paramasivam, M. Sasikala, T. Tamilam and A. Sumithra, *J. Entom. Zoology.* 2017.
- 11.L. Okerman, J. Van Hende and L. De Zutter, *Anal. Chem. Acta.* 2007, **586**, 284288.
12. C. W., Metters, J. P. and Banks, C. E. *Ult. Flex. Electrochem. Sens.* 25: 2275–2282.
13. K. Horner and P. Karadakov, *J. Org. Chem.* 2013, **78**, 8037-8043.
14. G. Minetto, L. Raveglia and M. Taddei, *Org. Chem.* 2004, **6**, 389-392.

15. D. Plausinaitis, L. Sinkevicius, L. Mikoliunaite, V. Plausinaitiene, A. Ramanaviciene and A. Ramanavicius, *Phys. Chem.* 2017, **19**, 1029-1038.
16. D. Bailey, R. Johnson and U. Salvador, *J. Med. Chem.* 1973, **16**, 1298-1300.
17. A. Castro, G. Gale, G. Means and G. Tertzakian, *J. Med. Chem.* 1967, **10**, 29-32.
18. S. Casadio, J. W. Lowdon, K. Betlem, J. T. Ueta, C. W. Foster, T. J. Cleij, B. van Grinsven, O. B. Sutcliffe, C. E. Banks and M. Peeters, *Chem. Engin. J.* 2017, **315**, 459-468.
19. B. Geerets, M. Peeters, B. Grinsven, K. Bers, W. de Ceuninck and P. Wagner, *Sens.* 2013, **13**, 9148.
20. NOVA 2.0, <https://www.metrohm.com/en-us/products-overview/electrochemistry/nova/> (accessed July 2017).
21. G. Li, Y. Wang and H. Xu, *Sensors*, 2007, **7**, 239-250.
22. A. Cascalheira, S. Aeiayach, J. Aubard, P. Lacaze and L. Abrantes, *Russian J. Electrochem.* 2004, **40**, 294-298.
23. Phosphate buffer saline: *Phosphate buffered saline tablets (PBS) were purchased from Sigma Aldrich. Phosphate-buffered saline (PBS) is a buffer solution used in biological research. It is a water-based salt solution containing sodium phosphate, sodium chloride and, in some formulations, it contains potassium chloride and potassium phosphate. The osmolality and ion concentrations of the solutions match those of the human body (isotonic) and are non-toxic to most cells.*
24. Bannanakere N. Chandrashekar, Bahaddurghatta E. Kumara Swamy, Mundargi Pandurangachar, Tammanekar V. Sathisha, Bailure S. Sherigara,

Electrochem. Invest. of 4-Aminophenol. 2010 ,**15** , 53-59.

25. Brief Introduction to Coating Technology for Electron Microscopy <http://www.leica-microsystems.com/science-lab/brief-introduction-to-coating-technology-for-electron-microscopy/>, (accessed September 2017).
26. H. ENSIKAT and M. WEIGEND, *J. Micros.* 2014, **256**, 226-230.
27. Emstat, <https://www.palmsens.com/product/emstat/>, (accessed October 2017).
28. PSTrace, <https://www.palmsens.com/product/palmsens4/#techniques>, (accessed October 2017).
29. R. Jones, *Chem. Heterocyc. Comp.* John Wiley & Sons, Canada, **1**, 2009.
30. *The preparation of the NIP and MIP of the antibiotic was carried out by me demonstrating to Jessica Pimlott, batch rebinding was done completely by her.*

Jessica has given me permission to use the data to contrast the graph in figure 51.
31. FTIR analysis, <https://www.labtesting.com/services/polymer-testing/ftiranalysis/>, (accessed October 2017).
- 32 . White Light Scanner, <https://www.scribd.com/document/342533883/WhiteLightScanner>, (accessed October 2017).
33. D. Yongabi, M. Khorshid, P. Losada-Pérez, K. Eersels, O. Deschaume, J. D'Haen, C. Bartic, J. Hooyberghs, R. Thoelen, M. Wübbenhorst and P. Wagner, *Sens. Actua. B: Chem.* 2017, 255, 907-917.

Figure references

Figure 1: M. Gama, C. Beatriz and G. Bottoli, *Journal of Chromatography B*, 2017, 1043, 107-121.

Figures 2, 3 and 4: *Picture taken using a light microscope*

Figures 5, 6, 9, 10 and 11: *all drawn using CHEMDRAW*

Figures 7 and 8: *captured using the camera on galaxy s6 phone*

Figure 8: Procedure: provide reference Foster, C. W., Metters, J. P. and Banks, C. E. (2013), Ultra Flexible Paper Based Electrochemical Sensors: Effect of Mechanical Contortion upon Electrochemical Performance. *Electroanalysis*, 2013, **25**, 2275–2282.

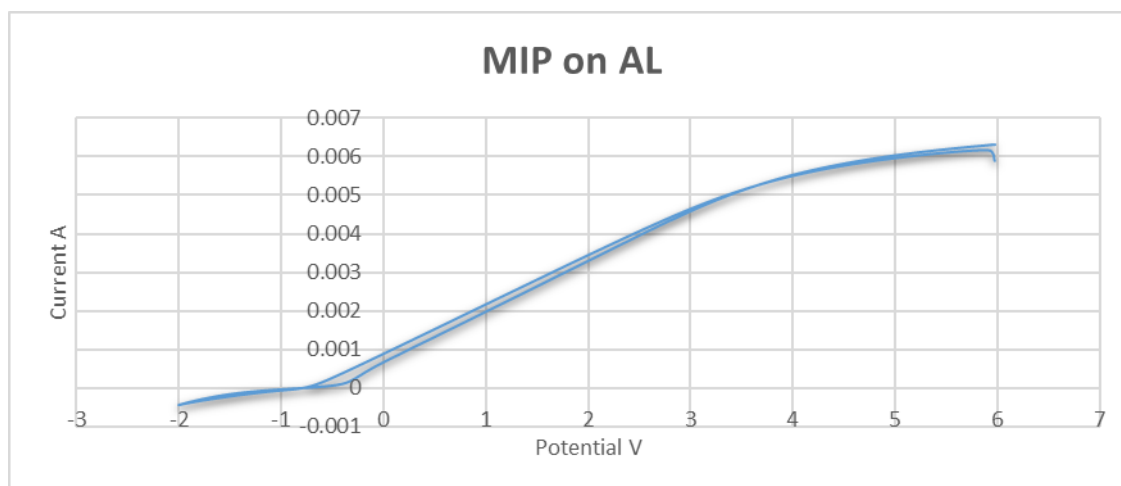
Figure 12: B. van Grinsven, N. Vanden Bon, H. Strauven, L. Grieten, M. Murib, K. L. Jiménez Monroy, S. D. Janssens, K. Haenen, M. J. Schöning, V. Vermeeren, M. Ameloot, L. Michiels, R. Thoelen, W. De Ceuninck and P. Wagner, *ACS Nano*, 2012, **6**, 2712-2721.

Figures 25, 26 and 27: *captured using the white light scanner* **Figures**

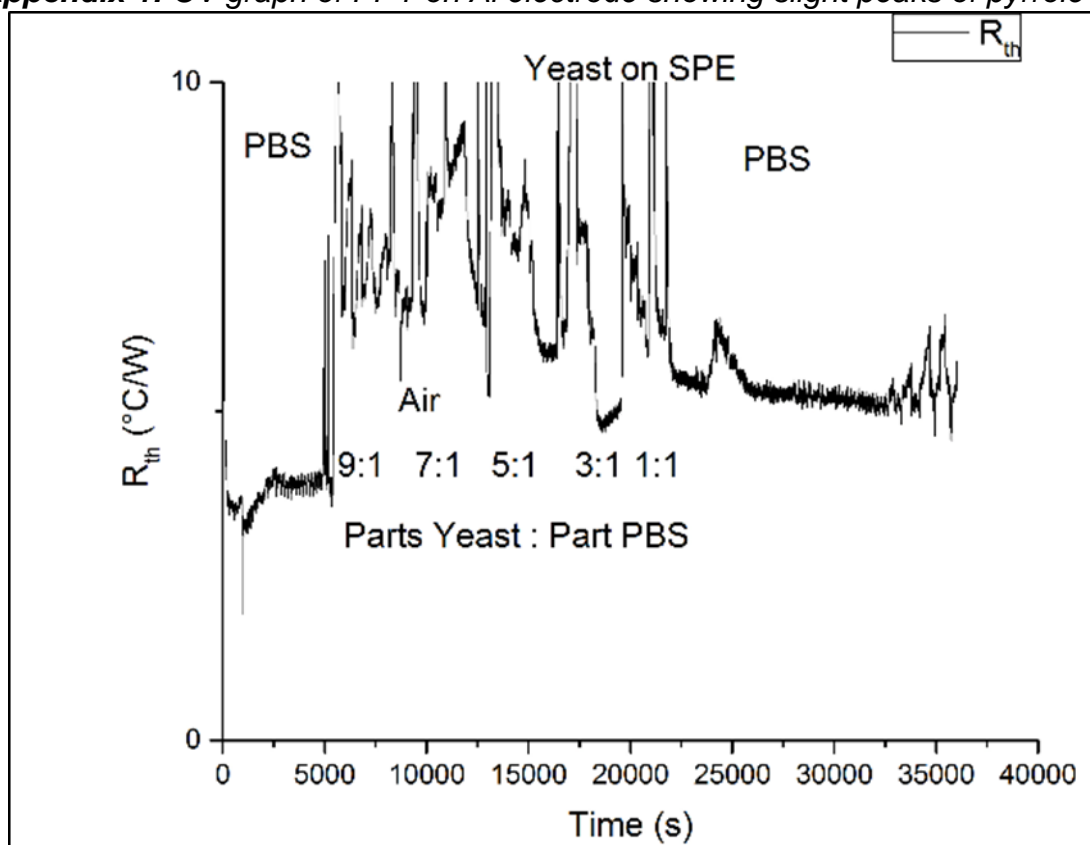
31, 32, 33, 34, 35, 36 and 37: *captured using SEM*

Figures 43, 44 and 45: *Picture taken using a light microscope*

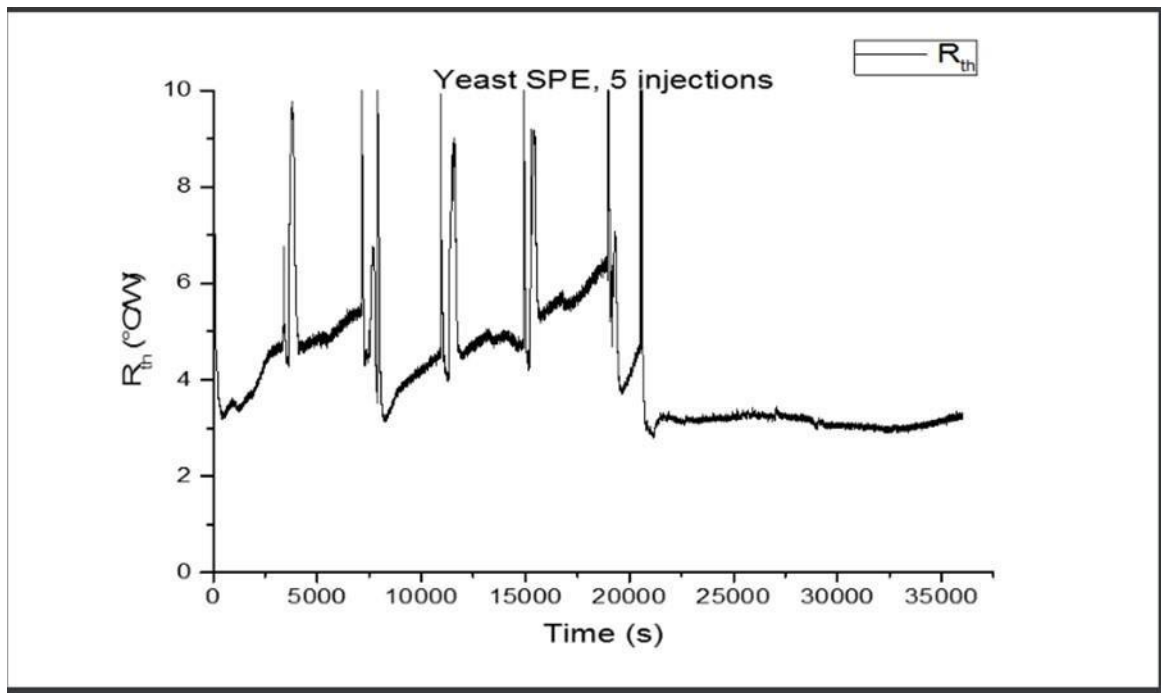
Appendix and Extra Information



Appendix 1: CV graph of PPY on Al electrode showing slight peaks of pyrrole

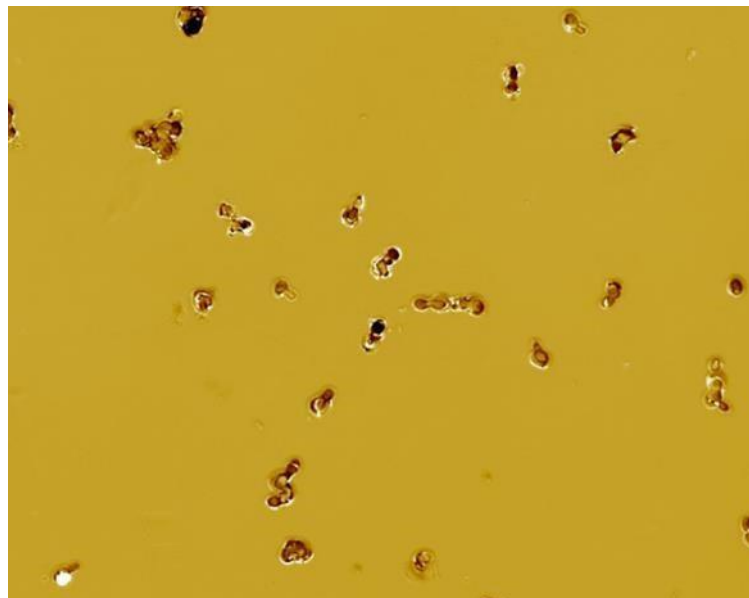


Appendix 2: Graph of HTM results, the injection pump was faulty and caused too many signals, making it problematic to determine which the authentic yeast signal was.

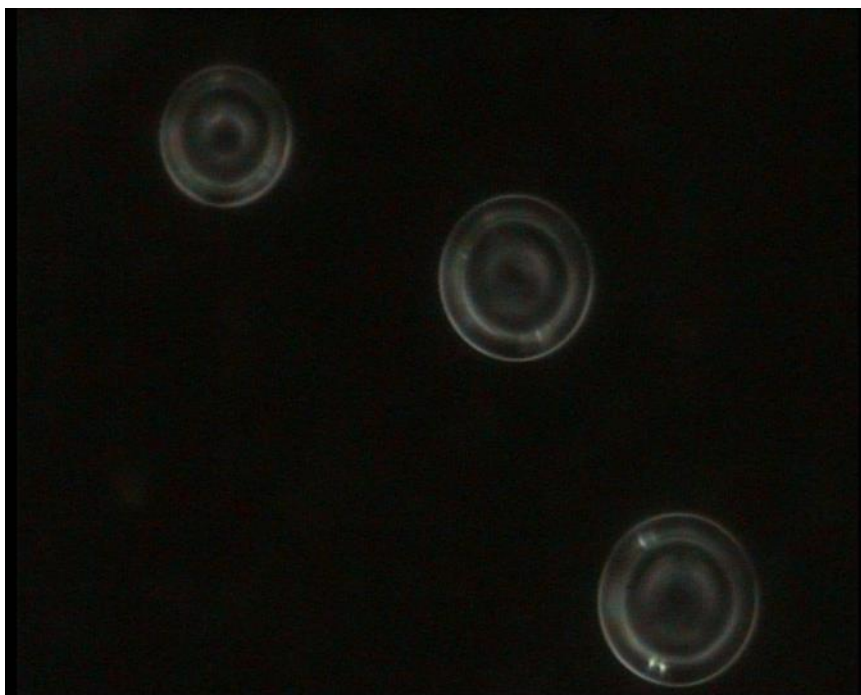


Appendix 3: *HTM data of when the system was not able to stabilise initially making it difficult to see if there were any increase in the signals after injections.*

System firstly injected with PBS then followed with five increasing injections of yeast and finally PBS was added again to wash the flowcell.



Appendix 4: WLS image of yeast deposited on the surface of a gold electrode



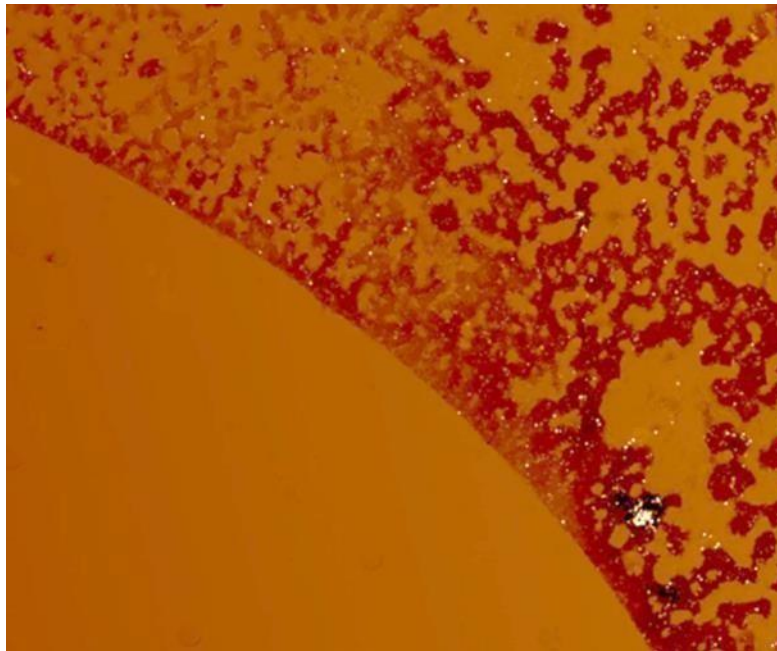
Appendix 5: Light microscope picture of yeast cells



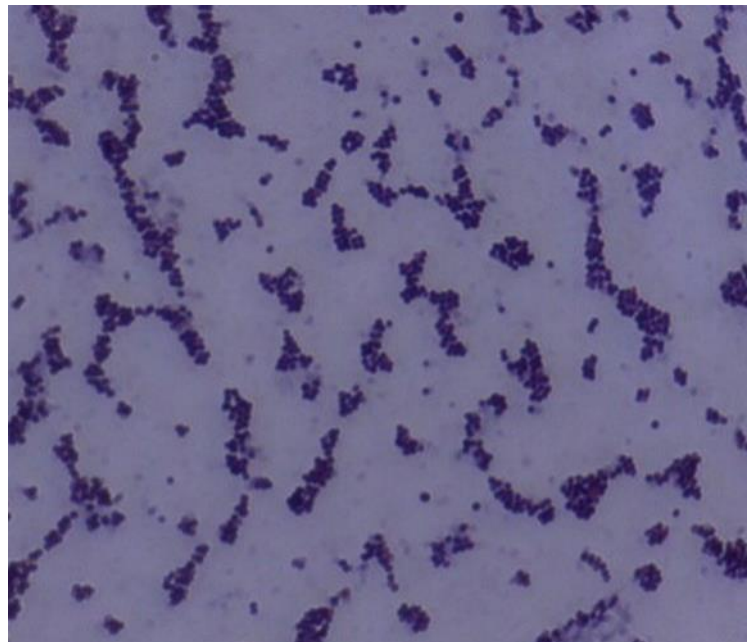
Appendix 7: Picture of yeast under the light microscope

After the yeast were extracted from the SPEs, the hot water used for the 2nd extraction was examined under the microscope to see whether yeast cells were

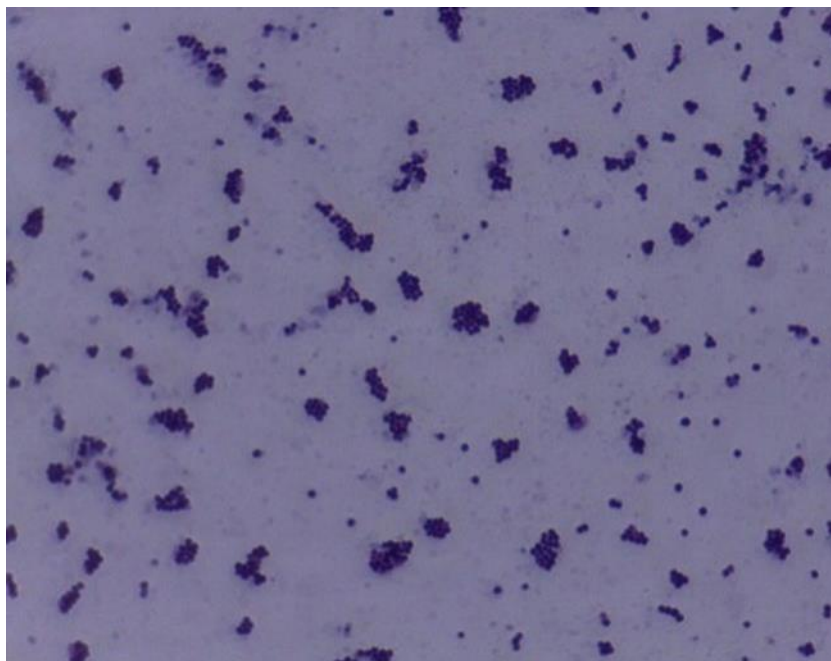
present and if they were still alive. The picture above is evidence that extraction has taken place and some yeast cells are still alive.



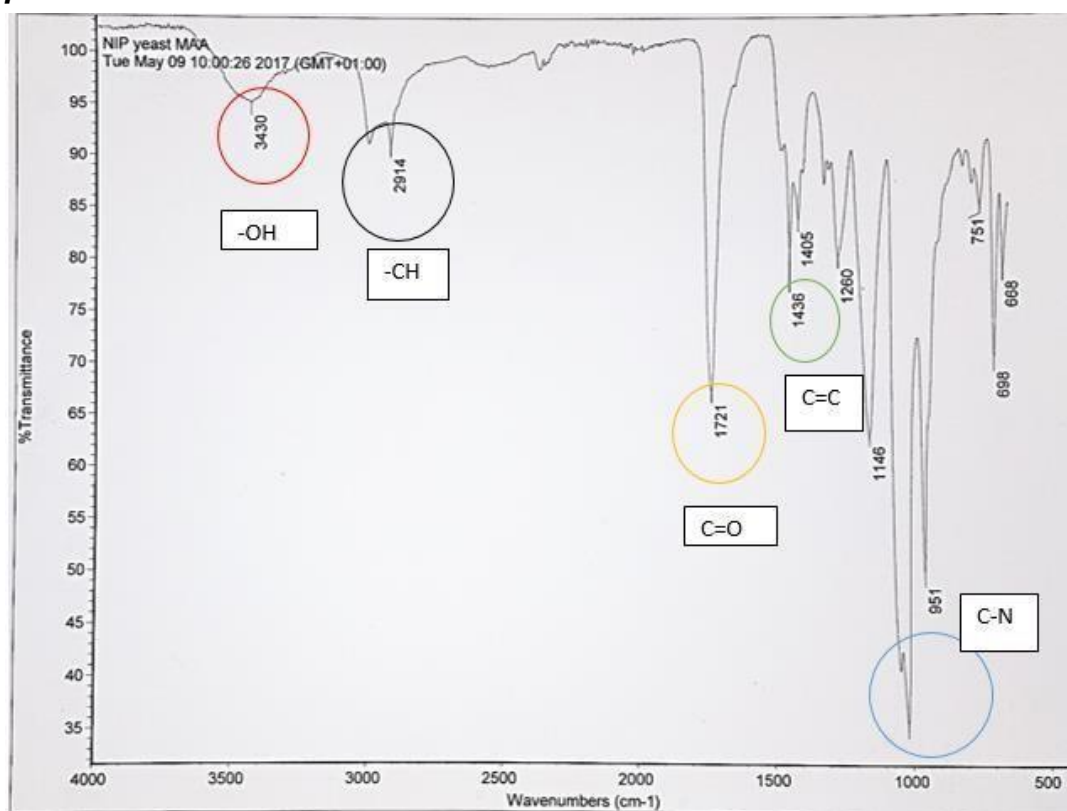
Appendix 8: MIP on gold electrode after extraction WLS



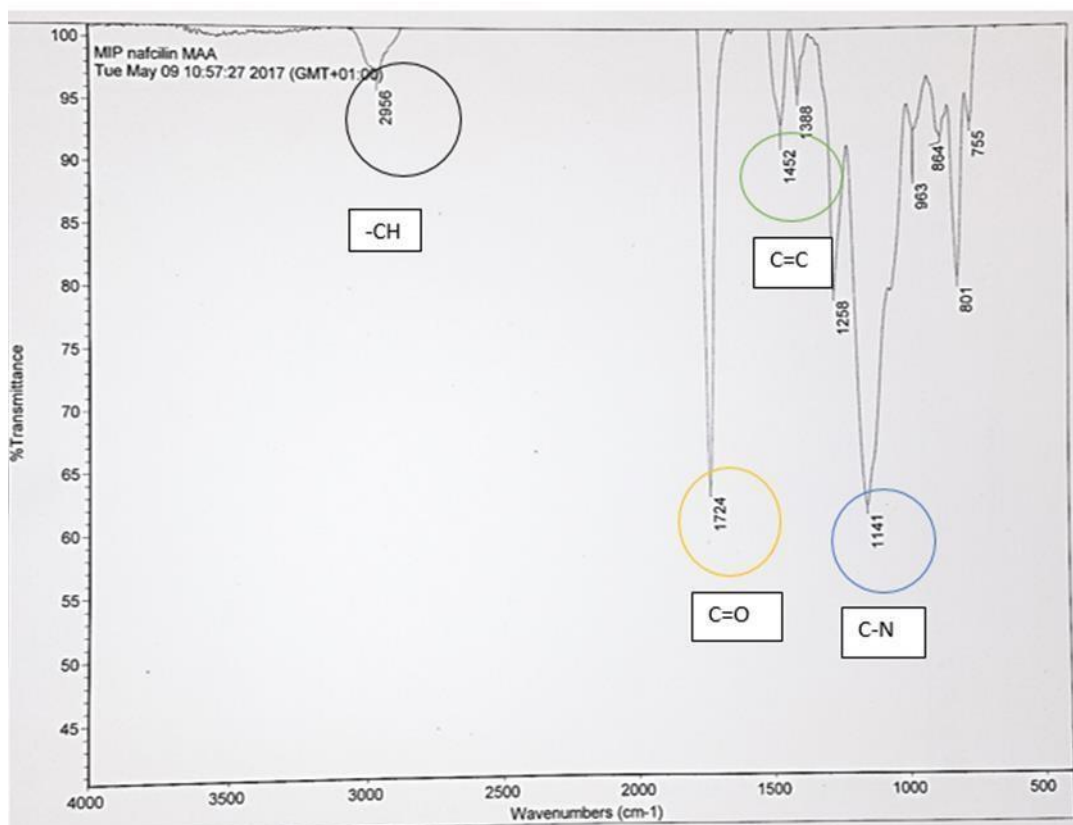
Appendix 9: Picture of MRSA strain C720



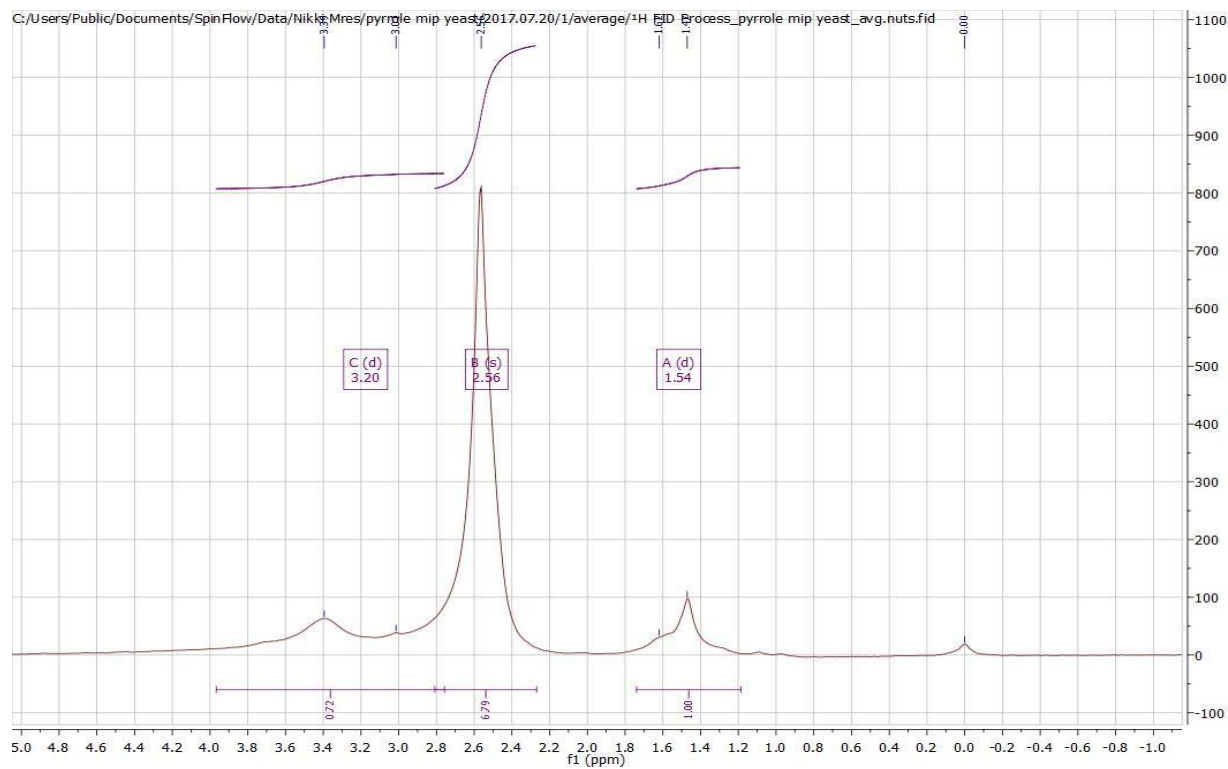
Appendix 10: Picture of MRSA strain C344



Appendix 11: IR results of bulk/ powder NIP of yeast synthesised with MAA



Appendix 12: IR results of NIP of Nafcillin synthesised with MAA



Appendix 13: NMR data of Pyrrole bulk MIP of yeast before extraction



Appendix 14: The counter electrode used for Potentiostat studies



Appendix 15: The reference Ag/AgCl electrode used during the Potentiostat studies



Appendix 16: Image of the Emsat used